MONITORING AND MODELING THE TERRESTRIAL SYSTEM FROM PORES TO CATCHMENTS

The Transregional Collaborative Research Center on Patterns in the Soil–Vegetation–Atmosphere System

BY CLEMENS SIMMER, INSA THIELE-EICH, MATTHIEU MASBOU, WULF AMELUNG, HEYE BOGENA, SUSANNE CREWELL, BERND DIEKKRÜGER, FRANK EWERT, HARRIE-JAN HENDRICKS FRANSSEN, JOHAN ALEXANDER HUISMAN, ANDREAS KEMNA, NORBERT KLITZSCH, STEFAN KOLLET, MATTHIAS LANGENSIEPEN, ULRICH LÖHNERT, A. S. M. MOSTAQUIMUR RAHMAN, UWE RASCHER, KARL SCHNEIDER, JAN SCHWEEN, YAPING SHAO, PRABHAKAR SHRESTHA, MAIK STIEBLER, MAURO SULIS, JAN VANDERBORGHT, HARRY VEREECKEN, JAN VAN DER KRUK, GUIDO WALDHOFF, AND TANJA ZERENNER

Observing and modeling the water and energy fluxes from soil pores to catchments and from groundwater to the atmosphere

BACKGROUND. State predictions for terrestrial systems are usually performed by means of numerical process models, which consider all compartments. However, it is unclear to what extent system heterogeneity must be considered for a particular set of conditions and for different types of model predictions. Numerical process models of the terrestrial system usually consider three vertically stacked media—representing the subsurface, including ground and surface water; vegetation; and atmosphere—that are typically coded in three separate compartment models. These compartment models interact at their

AFFILIATIONS: SIMMER—University of Bonn, Bonn, and Centre for High-Performance Scientific Computing in Terrestrial Systems (HPSC TerrSys), Jülich, Germany; THIELE-EICH, AMELUNG, DIEKKRÜGER, EWERT, KEMNA, LANGENSIEPEN, RAHMAN, SHRESTHA, SULIS, AND ZERENNER—University of Bonn, Bonn, Germany; MASBOU—Deutscher Wetterdienst, Offenbach; BOGENA, HUISMAN, RASCHER, VANDERBORGHT, VEREECKEN, AND VAN DER KRUK—Forschungszentrum Jülich GmbH, Jülich, Germany; CREWELL, LÖHNERT, SCHNEIDER, SCHWEEN, SHAO, AND WALDHOFF—University Cologne, Cologne, Germany; HENDRICKS FRANSSEN AND KOLLET—Forschungszentrum Jülich GmbH, and Centre for High-Performance Scientific Computing in Terrestrial Systems (HPSC TerrSys), Jülich, Germany; KLITZSCH—RWTH Aachen University, Aachen, Germany; STIEBLER—Technical University Braunschweig, Braunschweig, Germany

CORRESPONDING AUTHOR: Clemens Simmer, Meteorological Institute, University of Bonn, Auf dem Hügel 20, D-53121 Bonn, Germany
E-mail: csimmer@uni-bonn.de

The abstract for this article can be found in this issue, following the table of contents.
DOI:10.1175/BAMS-D-13-00134.1

Supplements to this article are available online (10.1175/BAMS-D-13-00134.2; 10.1175/BAMS-D-13-00134.3)

In final form 9 November 2014

mutual interfaces via fluxes of heat energy, water, carbon, nitrogen, and momentum, which are related to the state variables of the terrestrial system. For the atmosphere these include temperature, wind, density, pressure, and specific humidity of air. State variables of the subsurface are soil temperature and soil water content, but also the soil and aquifer water temperatures and the amounts of carbon and nitrogen in their different chemical forms. The state variables of the vegetation compartment include the temperature and internal water content, but also variables that describe the extent and structure of the interface with the atmosphere, such as leaf and stem area indices, and with the soil, such as the root length density.

Process formulations often rely on so-called parameterizations that replace complex small-scale processes with macroscopic simplified descriptions. These descriptions typically contain additional quantities that we refer to as parameters, which need to be determined empirically. The dependence of simulated energy and matter flow—and thus the evolution of the state variables—on such parameters differs considerably for the different compartment models. Atmospheric models require such parameterizations mainly for turbulent mixing, radiation interactions, and phase changes in clouds. However, many soil models rely much more strongly on parameterization because of the simplified representation of water flow in a porous medium using the Richards equation (Richards 1931). Vegetation models are almost exclusively based on parameterizations, and they also have to deal with the additional challenges associated with human actions to manage vegetation, such as sowing, harvesting, and irrigation.

Many patterns of terrestrial state variables and exchange fluxes between the compartments relate to the relatively static and often extremely heterogeneous parameters, which describe the soil and the subsoil. The latter has been generated on geological time scales and is additionally influenced by land-use management for centuries. The fast-moving and fast-mixing atmosphere drives—and is driven by—these fluxes, and adds considerable heterogeneity through its own internal scales of motion ranging from turbulence to convection and synoptic systems. The added atmospheric variability feeds directly back to the driving radiative—and ensuing heat—fluxes through clouds and water vapor and to water fluxes via precipitation. Vegetation also affects these fluxes and dynamically responds to the states of subsurface and atmosphere; it can be seen as a living transmission medium and is strongly subject to human interaction through agricultural and forest management and land-use change.

TerrSysMP

TerrSysMP (Fig. SB1; Shrestha et al. 2014) couples the hydrological model ParFlow (e.g., Kollet and Maxwell 2008; Kollet et al. 2010); the land surface scheme CLM, version 3.5 (Oleson et al. 2008); and the weather forecasting and regional climate model COSMO (e.g., Baldauf et al. 2011) using the OASIS3–MCT coupler (Valcke et al. 2012, 2013). The code has been ported to the massively parallel Blue Gene/Q supercomputing environment of the Jülich Supercomputing Centre (Gasper et al. 2014) in order to allow for high-resolution simulations over large areas. OASIS uses a dynamical two-way approach including downscaling and upscaling algorithms for fluxes and state variables between computational grids of different resolution (Shrestha et al. 2014). The upscaling algorithm uses the mosaic approach (Avissar and Pielke 1989; Ament and Simmer 2006; Mengelkamp et al. 2006) in which high-resolution land surface fluxes are averaged to the coarser atmosphere resolution before they are passed over to the atmospheric model. A downscaling scheme following Schomburg et al. (2010, 2012) is implemented that downscales atmospheric variables of the lowest layer to the higher-resolved land surface model. The scheme involves spline interpolation of the coarse field, deterministic downscaling rules via empirical relationships, and additive noise (see main text). All component models can be run in stand-alone mode or arbitrary coupled mode. When CLM is coupled with ParFlow, both models share the same upper soil layers. ParFlow takes over the hydrological calculations, while sources and sinks by rainfall and evapotranspiration are provided by CLM. The simulation in Fig. SB1 shows the 3D distribution of the relative soil saturation along with the turbulent eddy heat fluxes. A clear spatial structure can be observed at the land surface, with topographic convergent zones (i.e., river corridors) experiencing higher saturation values. In the atmosphere, patterns seem mainly controlled by the vegetation distribution. For instance, higher values of turbulent eddy fluxes can be identified over forested areas characterized by higher sensible heat fluxes. This can be explained by the increased available energy (via lower albedo) over such areas compared, for example, with crops. Note also that this effect tends to be amplified over steeper terrain with its lower level of soil saturation due to a more efficient lateral drainage. Currently, tests are carried out 1) with additional plant functional types for winter wheat and sugar beet (Sulis et al. 2015) in the CLM to better address the regional land-cover heterogeneity, 2) with interactive CO_2 land surface–atmosphere exchange and atmospheric transport, and 3) the inclusion of soil water convective heat energy transport in ParFlow.

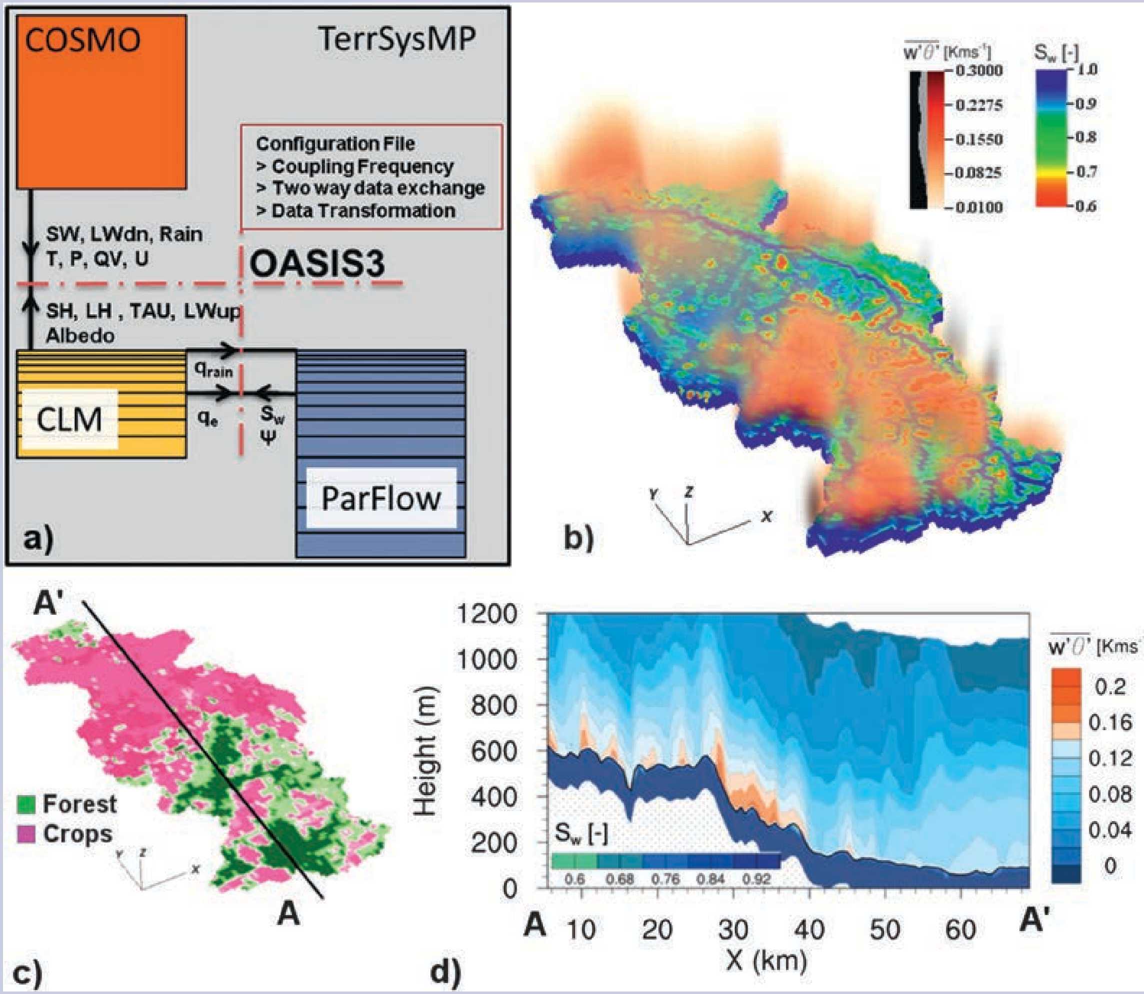

Fig. SB1. (a) Schematic of TerrSysMP [modified after Shrestha et al. (2014)] showing the fluxes and state variables exchanged between the three model components: COSMO (atmosphere), CLM (land surface and subsurface), and ParFlow (subsurface hydrology) via the OASIS coupler. SW, LWdn, Rain, *T*, *P*, QV, and *U* are passed from COSMO to CLM, while CLM passes back SH, LH, TAU, LWup, and albedo. CLM shares the upper soil layers with ParFlow within which q_{rain} and q_e are passed from CLM to ParFlow, which transmits back S_w and Ψ. (b) Turbulent eddy heat flux and relative soil saturation (nondimensional) along the Rur catchment. (c) Main land-use classes in the catchment. (d) Meridional cross section of turbulent eddy heat flux and relative soil saturation.

The pervasive heterogeneity of terrestrial systems makes monitoring and predicting state variables highly challenging tasks. Improving our understanding and prediction capabilities of the terrestrial system therefore requires measurement techniques that allow us to characterize and monitor the spatiotemporal evolution of system properties across scales, terrestrial system model platforms that include all relevant processes, and state variable assimilation and parameter estimation methods. The related challenges, which were very thoughtfully summarized and discussed by Lyon et al. (2008), were the starting point of CRC TR32 (www.tr32.de, see the appendix for acronym expansions), which deals with “Patterns in the soil–vegetation–atmosphere system—Monitoring, modeling, and data assimilation.” TR32 started in 2007 and includes a graduate school for doctoral students and a data management system (Curdt et al. 2012; see www.tr32db.uni-koeln.de) where all observations, analyses, and documents are stored for at least a decade. A central effort of TR32 is the development of the new terrestrial system modeling platform TerrSysMP (see sidebar on "TerrSysMP" for more information; Shrestha et al. 2014) applicable for regions ranging from typical mesoscale catchments (several thousand square kilometers) to the regional climate scale. TerrSysMP couples different state-of-the-art compartment models for the simulation of water, carbon, and energy flow in the terrestrial system from the interactive groundwater to the atmosphere. Developments focused on the two-way coupling of the compartment models while honoring the spatial and temporal scales on which the exchange processes take place.

German CRCs. CRCs are established at German universities and cofunded by the German national science foundation (DFG) for a period of up to 12 years subdivided into three phases (www.dfg.de/en/research_funding/programmes/coordinated_programmes/collaborative_research_centres/index.html). Each CRC phase is funded based on applications that need to be positively evaluated in a two-step approach. The first step consists of a review by an international panel, and the second step involves a highly competitive evaluation procedure that assesses and compares proposed CRCs from all research fields. CRCs enable researchers to pursue long-term outstanding research programs that typically cross disciplinary and institutional boundaries. The CRC program in turn contributes toward defining and sharpening the university profile with respect to research as well as teaching. CRCs may incorporate projects at nonuniversity research institutions and collaborations with government agencies and industry. While CRCs are usually applied for by a single university, the TR32 is a so-called transregional CRC, in which the universities of Bonn (leading), Cologne, and Aachen, and the Forschungszentrum Jülich GmbH of the Helmholtz Association join their efforts to better understand the origin and propagation of patterns in the terrestrial system through measurements and modeling.

Patterns in system parameters and state variables. The TR32 focuses on the role of spatial patterns, including their dynamics for observation and modeling the terrestrial system, as reflected in the state variables and system parameters of terrestrial system models. Patterns may be understood as repetitions of similar structures in system state variables and system parameters in space and time. Structures denote identifiable objects, like a single soil pore, a plant root, an individual plant, a plough mark, soil heterogeneity associated with a paleoriver system, a crop-cultivated field, a single hill, or an entire valley, most of which will be reflected in parameters of terrestrial system models. Typically, these structures create patterns that are rather static relative to the time scales on which fluxes vary within or between compartments. However, patterns can also be more dynamic, as in the case of the response of soil temperature and moisture to insolation or precipitation, and any structure in the atmosphere ranging from single eddies, to updrafts in the ABL, to cumulus clouds, to thunderstorms, and to cyclones. Most, if not all, of these structures and resulting patterns have characteristic scales on which they can be detected, but often they integrate out when enlarging the observation scale. Examples are cumulus clouds and cultivated fields, which are small in many regions, whose characteristic patchy and rectangular shape, respectively, visually disappear when the spatial resolution significantly exceeds the 100-m scale. Of course, this does not mean that these small-scale patterns become irrelevant for surface flux estimation at larger scales. But reliable scale variance relations for the estimation of smaller-scale variability from larger scales, for example, in the inertial subrange of turbulent motion (Kolmogorov 1941), usually do not apply.

TR32 develops and applies terrestrial system models for state simulations from minutes to years and analyzes the role and importance of these patterns for flux estimation and system predictability. On these time scales, system parameters of the soil are usually assumed to be constant, whereas states of, for example, the ABL, are predictable from the state variables and land surface characteristics. As discussed above, the distinction between system parameters and state variables is a concept born out of the model perspective: parameters refer to parameterizations of processes that evade direct numerical simulation using first-principle equations for the conservation of mass, energy, and momentum due to the required but computationally unattainable high resolution. Nevertheless, homogeneity assumptions are commonly invoked for the soil and atmosphere in order to justify parameterization concepts such as the use of hydraulic conductivity in the Richards equation or the use of MOST (Monin and Obukhov 1954) of the ABL in RANS models (e.g., Chen et al. 1990). All parameters do actually vary, not only with the numerical resolution of the models due to the natural variability and the nonlinearity of the processes, but also with time because they depend on the system state variables, their subgrid variability, and possibly also their history (hysteresis effects). In atmosphere models, most parameters can be estimated from state variables by involving turbulence theory, known as the closure problem (e.g., Mellor and Yamada 1982). In subsurface models, the porous medium, for instance, is parameterized at the macroscopic or Darcy scale using the hydraulic conductivity and the water retention characteristic, which are usually estimated or deduced from experiments (Bear 1988). In both cases parameters can also be estimated from higher-resolution models (e.g., LES models for the atmosphere, and pore-scale models for the soil; see "Modeling the terrestrial system on different scales" section). This implies that there is no clear-cut distinction between system parameters and state variables, which is a problem that is also increasingly recognized in data assimilation.

TR32 employs the pattern paradigm as an overarching concept to address the ubiquitous upscaling and downscaling issues in monitoring, modeling, and data assimilation. We hypothesize that the explicit consideration of patterns will pave the way toward a common interdisciplinary methodological framework that will increase our understanding of terrestrial system functioning.

While patterns are sometimes considered within compartmental models, they are usually ignored in models that cross compartmental boundaries. Prominent examples are the use of a limited number of weather station datasets for one-way forcing of hydrological models or the omission of subgrid spatial patterns of land surface characteristics (in addition to their probability density functions as considered in the tile approach) of the lower boundary in weather and climate models (Avissar and Pielke 1989; Koster and Suarez 1992; Ament and Simmer 2006). More detailed information on this topic can be found in Vereecken et al. (2010).

We acknowledge the huge existing body of literature on patterns and pattern development in the geosciences. Examples are diverse multifractal scaling laws following from physical concepts like self-organized criticality (Bak et al. 1988) or constructal theory (Bejan and Lorente 2006), which nicely explain the generation of flow systems in homogeneous media as the result of an optimization. Many processes within the compartments of the terrestrial system follow such concepts and exhibit the predicted patterns. Close to the interfaces, however, the connecting processes are subject to patterns generated from different systems including human interaction, which do not have much in common. Studying how patterns influence fluxes and state variables, especially at the compartment boundaries across scales, is a key goal of the TR32.

Theoretically, the most appropriate way for modeling the terrestrial system requires its treatment as a continuum with spatial resolutions that allow the simulation of all relevant flow processes by the Navier–Stokes equations using DNS models down to the subpore scale, which reduces the exchange at compartment boundaries with diffusive processes. This would also take into account small-scale processes such as the movement of plants in the turbulent airflow and water motion in pores. Patterns would not need to be considered in this approach, as they turn up automatically as a natural consequence of the acting processes. However, the use of such DNS models at these scales is computationally prohibitive; requires extensive datasets, which may not be available; and demands mathematical algorithms and relationships that are beyond current scientific understanding. Instead, bulk modeling approaches are used, such as the Richards equation for flow of water in soils, which captures microscale pore geometry in two macroscopic material properties: the water retention and hydraulic conductivity functions. Pore-scale models are used in TR32 to understand and derive these bulk properties. The atmosphere is usually simulated using RANS models, which use the time-averaged Navier–Stokes equations and treat the effects of the nonresolved variability of the state variables on the averaged state variables by closure assumptions from turbulence theory. All weather prediction and climate models are based on this approach, which requires especially strong assumptions near boundaries usually tackled with MOST. As a consequence, the exchange between system compartments is parameterized by diffusion-like processes with coefficients and material properties estimated from experiments and/or statistics of the larger-scale flow like its mean vertical gradient. This is where patterns that are not resolved by one or both compartment models become important: since the exchange between compartments is driven by local gradients of state variables, any correlation between their spatial and temporal patterns at the boundaries (e.g., temperature at the surface and the lowest atmospheric model layer) will directly impact the fluxes, possibly induce other flux-relevant flow phenomena (e.g., dust devils at the boundary between different land uses or internal waves in the boundary layer), and thus impact the system state evolution. Thus, patterns are an inevitable element of any upscaling and downscaling concept applied in terrestrial system modeling, a quest taken up by TR32 and illustrated in the remainder of this paper.

MONITORING OF THE RUR CATCHMENT. The development of techniques to map and understand patterns, and to use this to model and predict the terrestrial system, requires a real counterpart for analysis and testing. TR32 identified the Rur catchment (Fig. 1) as its central observation site because

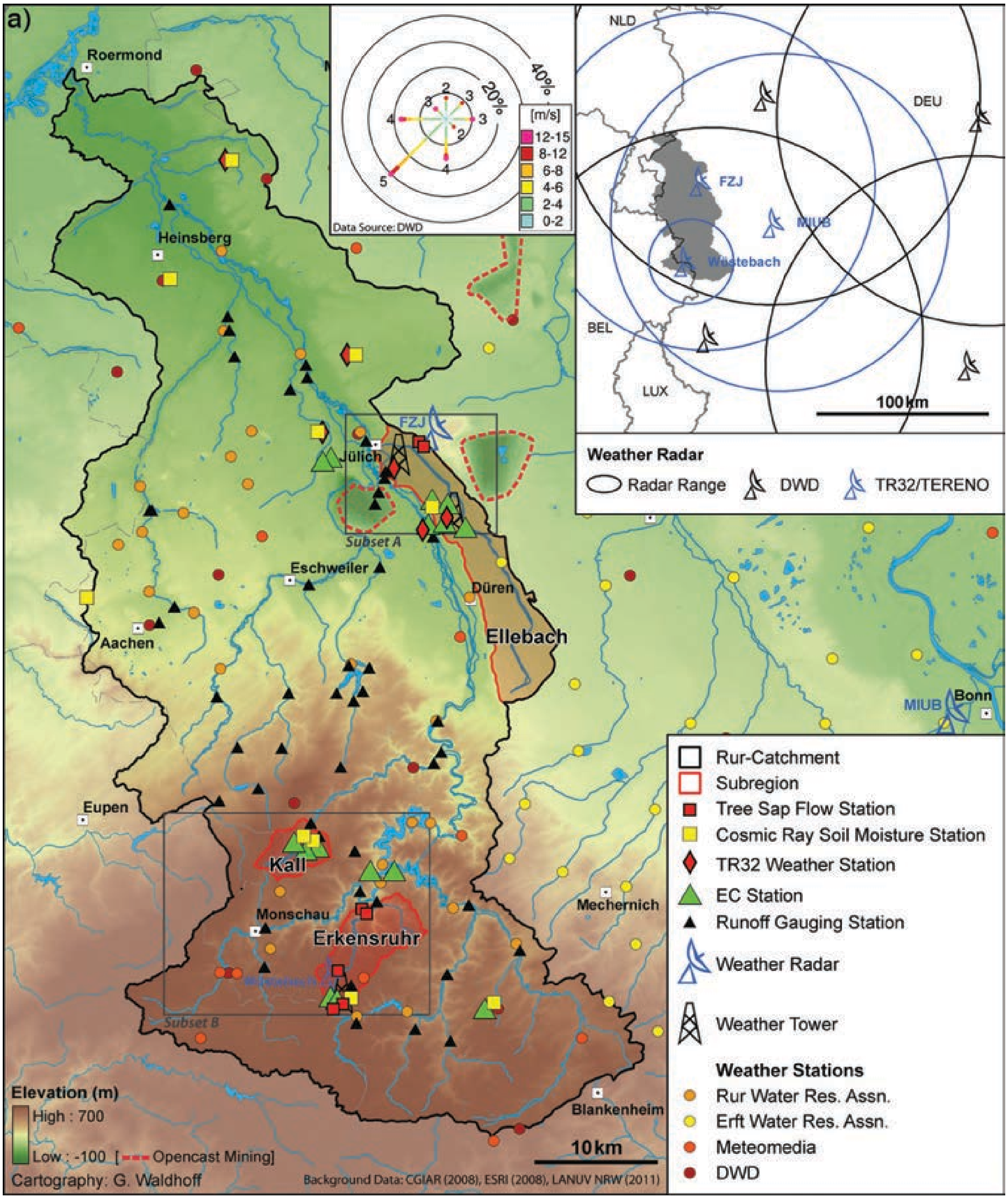

Fig. 1a. Map depicts the Rur catchment including the position of monitoring devices like weather, river gauging, EC, and cosmic-ray stations, as well as a polarimetric weather radar coverage inset for TR32 [X-band radar BoXPol at Meteorological Institute of the University of Bonn (MIUB)]; TERENO [X-band radar JuXPol at Forschungszentrum Jülich GmbH (FZJ)]; and the surrounding C-band radars of DWD, including the nonpolarimetric Rainscanner at Wüstebach and other instrumentation. Active and remnants of open-pit mines are delineated by dashed red lines. The wind rose inset at the top is based on hourly observations of DWD at the weather station Aachen (about 200 m MSL) at the western edge of the catchment for the years 2008–13. The mean wind speed is printed at the end of the eight directional lines. Each circle represents the percentage of time the wind comes from that direction, while the colors indicate the respective discretization into wind speed intervals.

of its strong diversity with respect to weather, soil types, and land use. Monitoring of a river catchment simplifies the budgeting of water flows by discharge observations and provides valuable information for data assimilation into terrestrial models. The Rur catchment covers a total area of 2,354 km^2 with about 2,088 km^2 (88.7%) in western Germany, 157 km^2 (6.7%) in Belgium, and about 108 km^2 (4.6%) on Dutch territory. German catchments of this size are often managed by dedicated governing boards, and are comparable in size to the typical administration aggregation level (Kreis) above single villages and cities. Thus, monitoring and modeling may eventually feed into applications for water and land-use management and flood prediction.

Weather in the Rur catchment is mostly influenced by southwesterly to northwesterly flow of relatively moist and temperate air masses from the North Atlantic. The multiyear average annual-mean temperatures range from 6°C in the Eifel range in the south to 10°C in the northeastern part of the catchment. Precipitation is on average rather evenly distributed over the year, while multiyear-mean annual precipitation ranges from about 600 mm in the east to 1200 mm in the south. Interannual variability of mean annual precipitation can be as large as ±30%. Approximately 53% of the near-surface rocks are formed from unconsolidated sediments, mainly quaternary deposits. Thick tertiary unconsolidated rock deposits in the region are mostly covered by

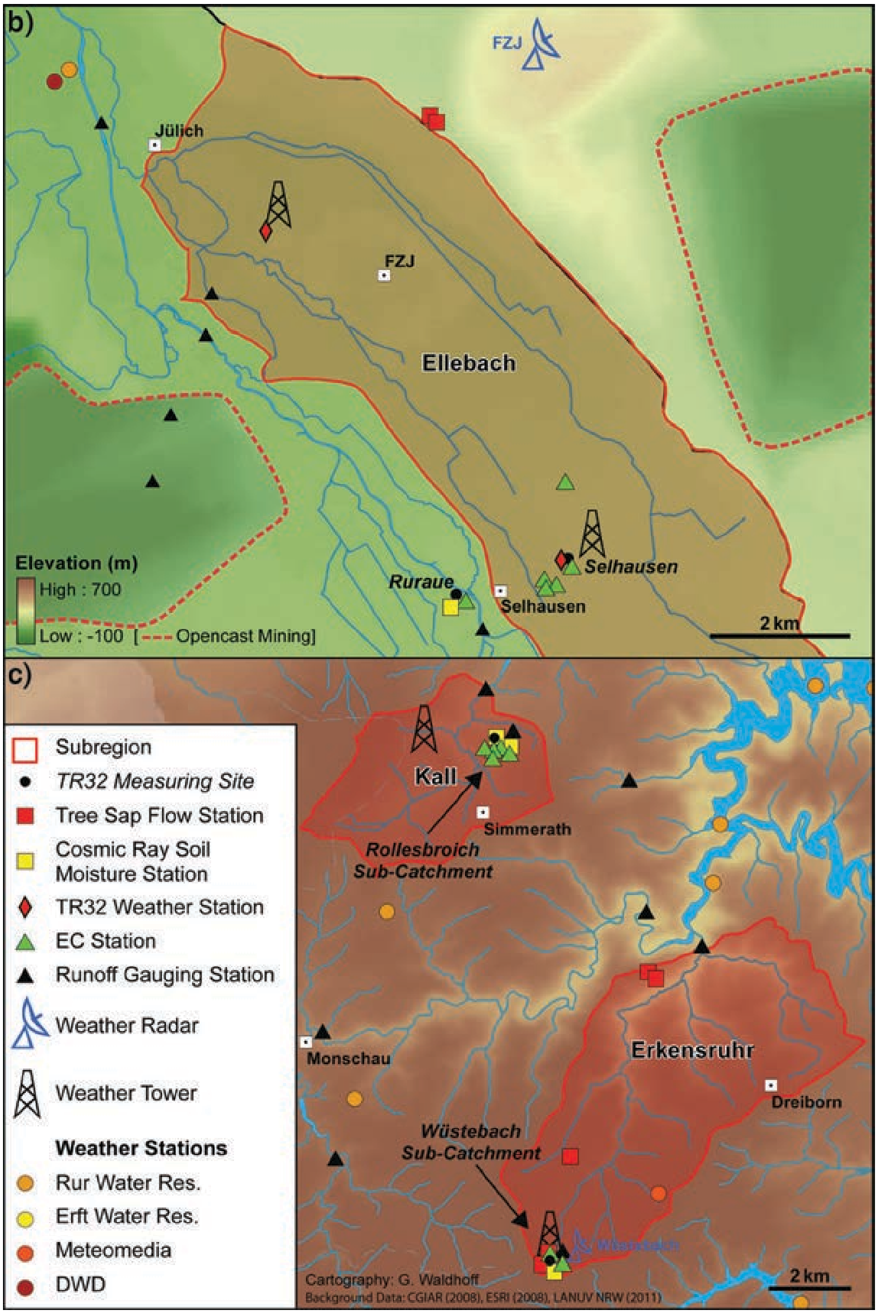

Fig. 1b,c. The three areas delineated in solid red in (left) are reproduced in higher resolution. These areas are subcatchments representing (b) crops (Ellebach subcatchment, including the Selhausen test site) and (c) forest (Erkensrur subcatchment, including the Wüstebach subcatchment) and pasture (Kall subcatchment, including the Rollesbroich subcatchment), which are more intensively monitored, for example, by soil moisture networks (Wüstebach and Rollesbroich subcatchments) or geophysical methods (Selhausen test site). The two river runoff stations west of the Ellebach catchment [see (b)] became obsolete due to river rerouting caused by recent open-pit mining activities.

Pleistocene terrace sediments and aeolian deposits. Large parts of the catchment are dominated by silty soil textures, with sandy soils dominating the extreme northern part of the catchment. The lowland region in the northern part is strongly urbanized and characterized by intensive agriculture, whereas the low mountain range in the southern part is sparsely populated and includes several drinking water reservoirs. Arable land mainly found in the northern lowland regions accounts for 37%, while forests cover a total area of 34% and dominate the upland region. Pastures account for 22% and are found mainly in the upland areas. Paved areas account for 5% and are mainly allocated in the north. Open cast mining has drastically changed about 1% of the area, predominantly in the east due to the accompanying significant extraction of groundwater in the region. This has a considerable impact on groundwater dynamics over much larger areas and on river flow in downstream regions.

The Rur catchment is monitored in strong cooperation between TR32 and the TERENO program of the Helmholtz Association (http://teodoor.icg.kfa-juelich.de; see Fig. 1), which was developed in parallel to TR32 as a network of catchment-based terrestrial observatories distributed over Germany (Zacharias et al. 2011). Within TERENO, changes in all compartments of the terrestrial system caused by climate change and human land surface management will be monitored for at least 15 years. The Rur catchment was selected because of its particularly strong gradient in and diversity of human interaction, which range from nature reserves to large cities, and because of its susceptibility to climate change.

The combined monitoring efforts of TR32 and TERENO turned the Rur catchment into a heavily instrumented region, quite similar to the Cooperative Atmosphere–Surface Exchange Study (CASES; LeMone et al. 2000). CASES, which was set up in 1997 for the Walnut River watershed (Kansas), was an early catchment-oriented approach toward monitoring the complex exchange processes between soil, vegetation, and atmospheric boundary layer. Heterogeneity in precipitation is the main driver of soil moisture patterns in the Rur catchment. Precipitation is continuously monitored at 5-min intervals by the twin dual-polarized X-band Doppler radars BoXPol in Bonn and JuXPol in Jülich on the Sophienhöhe (e.g., Ryzhkov et al. 2014), a hill created from open-cast mining and jutting roughly 200 m out of the surrounding terrain. A third reflectivity-only X-Band radar (Rainscanner) in the southwest measures at 1-min resolution. The area is also covered by four C-band radars of DWD, which have been recently upgraded to polarimetry to improve quantitative precipitation estimates and to differentiate between snow and rain. Precipitation patterns derived from sets of overlapping scanning radars are usually plagued with artifacts imposed by the observation method via beam clutter, beam blocking, and attenuation. Such effects are reduced by the so-called $R(A)$ methodology based on specific attenuation along the radar beam, developed by Ryzhkov et al. (2014) and extensively validated over the Rur catchment by Diederich et al. (2015a,b). Detailed information of the atmospheric state is available in near–real time from JOYCE (http://www.geomet.uni-koeln.de/en/research/joyce/; Loehnert et al. 2015), which is equipped with a unique array of state-of-the-art active and passive remote sensing and in situ instruments. The continuous and temporally highly resolved measurements focus on the ABL and allow the characterization of the diurnal cycle of turbulence, water vapor, stability, and cloudiness (Schween et al. 2011). JOYCE was developed from the efforts toward integrated cloud monitoring during the BALTEX BRIDGE campaign (Crewell et al. 2004) of GEWEX. A specific feature of JOYCE is the use of scanning measurements that are able to capture atmospheric patterns and their relation to the land surface (see http://dx.doi.org/10.1175/BAMS-D-13-00134.2). Fluxes of sensible heat, evapotranspiration, CO_2, and momentum are monitored by five fixed EC stations and by one roving EC station. The latter can be deployed on demand at different places for variable time periods in order to support, for example, the investigation of flux changes caused by land management changes or harvesting. Two typical subcatchments (the southernmost delineated areas in Fig. 1) representing forest (the Wüstebach catchment as part of the Erkensrur catchment) and pasture (the Rollesbroich catchment as part of the Kall catchment) are equipped with extensive wireless soil moisture networks with hundreds of sensors in various depths (Bogena et al. 2010), which allow for the examination of seasonal- and event-scale spatial soil moisture dynamics, the validation of models (Cornelissen et al. 2014; see also "Modeling the terrestrial system on different scales"), and remote sensing techniques like passive microwaves (e.g., Hasan et al. 2014). We found clockwise hysteretic soil moisture dynamics at the event scale during intense precipitation events that rapidly wetted the topsoil (Rosenbaum et al. 2012). Ten cosmic-ray soil moisture probes (Zreda et al. 2008) partially supplement the installed soil moisture networks (Bogena et al. 2013) for cross calibration (Baatz et al. 2014); they are distributed within the Rur catchment (see Fig. 1) in order to allow for the characterization of temporal soil moisture dynamics over the entire catchment in combination with indirect observations from space (Koyama et al. 2010; see below) using data assimilation techniques (see section 4). A suite of geophysical methods like NMR (e.g., Perlo et al. 2013), SIP (e.g., Kemna et al. 2012), EMI (e.g., Mester et al. 2011), and GPR (e.g., Busch et al. 2014) are employed at a few specific field-scale sites to develop and test methods for probing the structure and composition of the subsurface. The EMI and GPR systems are currently mounted on single- and multi-offset sleds pulled by an ATV and georeferenced using standard global positioning services like NAVSTAR GPS, GLONASS, and Galileo. Once the systems have been fully developed, we envision the use of programmed ATVs for monitoring larger areas. Recent results from the inversion of EMI observations [Fig. 2; for details, see von Hebel et al. (2014) and Rudolph et al. (2015)] showed a clear link between subsoil patterns of higher clay content originating from paleorivers (red dashed lines in Fig. 2e), which are characterized by high ECa values (Figs. 2b,c), the visual state of vegetation (Fig. 2d), and satellite-derived LAI (Fig. 2a) after an extended drought period. MRI, probably best known from medical applications (e.g., brain inspection), has been further developed in TR32 for soil applications in the laboratory and is currently being applied in the field to measure soil water content with high vertical resolution near the soil surface to improve the understanding of evaporation processes. Our observations also address ecosystem exchange processes on various scales for agricultural surfaces (e.g., Langensiepen et al. 2012). The role of soil patterns for soil carbon pools and soil heterotrophic respiration is analyzed using MIRS (Bornemann et al. 2010, 2011) and geostatistical modeling (Herbst et al. 2012), respectively. In several intensive measurement campaigns, aircraftborne instruments are used to measure the spatiotemporal structure of the ABL, including the CO_2 concentration, to analyze, for example, the relation between surface flux patterns and patterns of water vapor and CO_2 in the atmosphere (for an example, see http://dx.doi.org/10.1175/BAMS-D-13-00134.2). Vegetation, soil moisture, and land use over the whole catchment is derived by the combined use of state surveys, observations via aircraft and satellites, and in situ observations over selected fields (Hoffmeister et al. 2013; Koyama et al. 2010). Future efforts will include T_s observations (see the appendix for acronym definitions) and their diurnal changes in combination with model simulations to follow up on the study by Grossman et al. (2005), who relate spatial patterns in the relation between T_s and boundary layer air temperatures to catchment-scale boundary layer circulations induced by topography and spatiotemporal variability in land use and land management. Vegetation CO_2 assimilation activity states are observed using ground-based fluorescent-related techniques (Damm et al. 2011) and related airborne instrumentation that is a prototype for future space-based mission. Directional effects of the chlorophyll emission at the canopy level (van der Tol et al. 2009), terrain and flight height, as well as the viewing angle, have to be considered in the retrieval method (Damm et al. 2014a,b). Our observations (Fig. 3) document the large between-field and within-field variability of plant photosynthetic activity and may in the future be used for directly quantifying plant transpiration. Patterns have also been investigated within the soil moisture monitoring activities with a particular focus on the scaling properties of agricultural land (Korres et al. 2013). The dependence of evapotranspiration on soil states, soil and root properties, and meteorological conditions is analyzed using sap-flow devices installed on trees and crops. The sap flow of trees is measured in the Rur catchment at 30-min resolution in seven clusters of three trees each at four different sites (Fig. 1). The monitored tree species cover two clusters of spruce, one cluster of Douglas fir, and two clusters each of beech and oak. Results obtained in the Wüstebach subcatchment will be upscaled to the stand level and compared to EC-tower observations. Sap flow in wheat has been monitored since 2011 at 10-min intervals during the main growth periods at characteristic locations around Selhausen, Germany, including a field that contains two rhizotron facilities (see "Soil root model" for more information). These measurements were scaled up to the field level using information about tiller densities. The method was validated in 2011 and 2012 with independent measurements of latent heat flux in a field with homogeneous soil conditions at Merzenhausen, Germany, which was located at a distance of 20 km from the Selhausen site (Langensiepen et al. 2014). Wheat transpiration is upscaled to the Rur catchment using a Penman–Monteith-based modeling approach and information about ecophysiological crop responses to soil heterogeneity from sap-flow and leaf gas exchange measurements.

MODELING THE TERRESTRIAL SYSTEM ON DIFFERENT SCALES. TR32 employs a cross-scale, multicompartment modeling approach

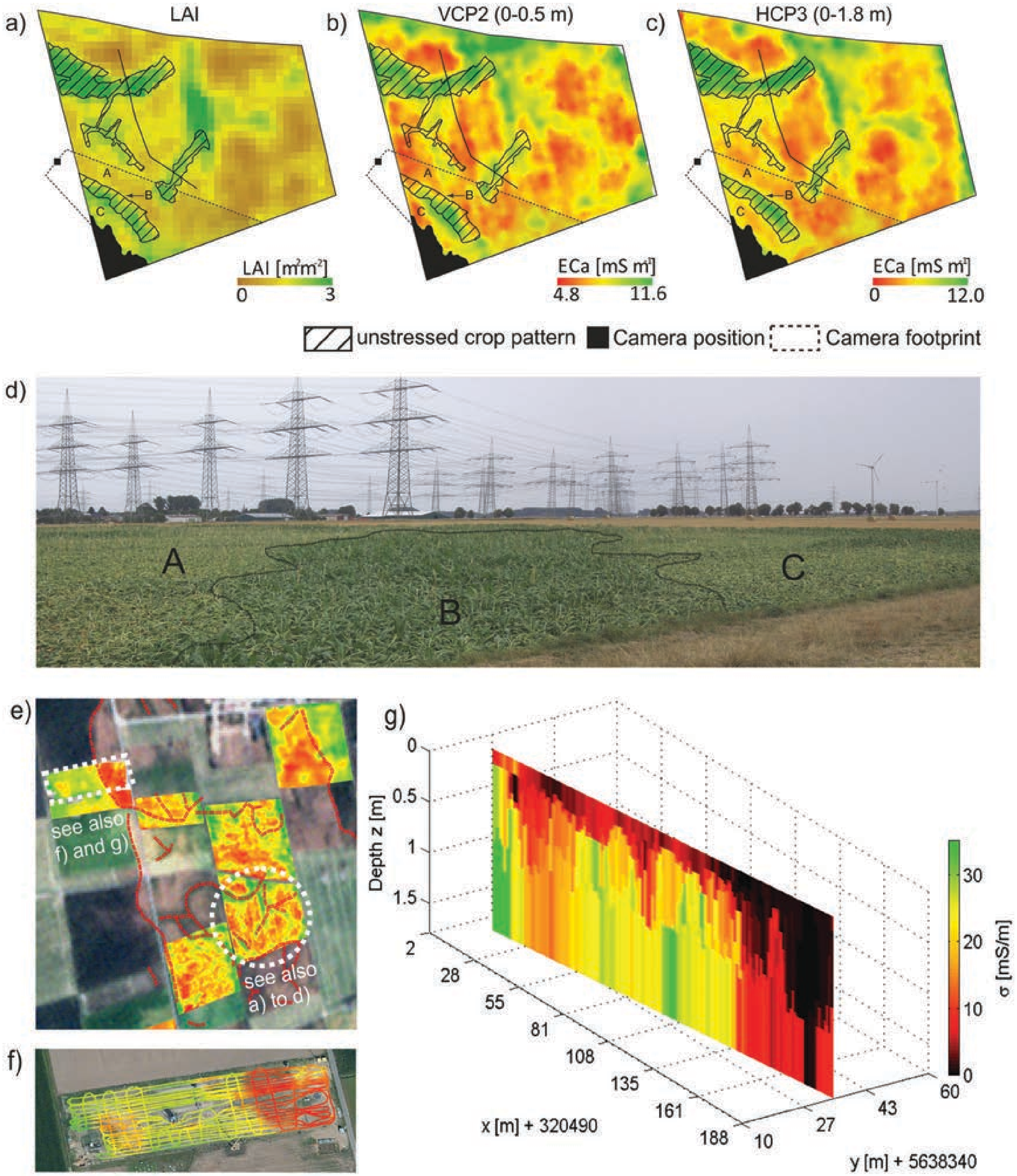

Fig. 2. (a) Satellite-derived LAI distribution in May 2011, estimated after a 2-month drought period over (e) the lower field encircled by a white dashed line. (b),(c) ECa measured by EMI with depth sensitivities down to 0.5 and 1.8 m, respectively, in Jun 2012. (d) Photo taken in Aug 2013 [camera position and view are delineated in (a)–(c); see symbols] indicates stressed (areas A and C) and unstressed (area B) regions in a sugar beet field. (e) ECa measurements for a larger area, with green colors indicating high values and red colors indicating low values. Red dashed lines indicate paleoriver channels. (f) Enlargement of the Selhausen test site, where the EMI measurement lines are clearly visible. The area is indicated in (e) by a white dashed rectangle. (g) Cross section of a quasi-3D EC distribution of the subsurface obtained by a three-layer inversion of multiconfiguration ECa measurements along the east–west direction of the Selhausen test site in (f) using a Maxwell forward model at every grid point [modified from von Hebel et al. (2014)].

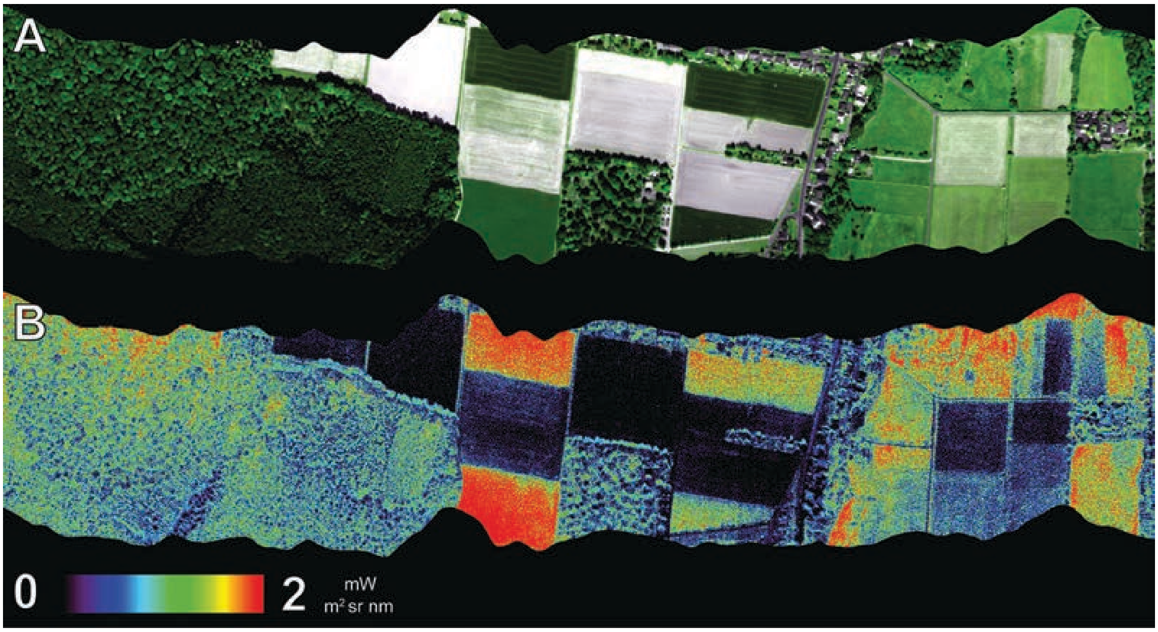

Fig. 3. Airborne observation (600 m AGL) of sun-induced fluorescence from Sep 2012 using the high-performance imaging spectrometer HyPlant. HyPlant allows for the quantification of the emitted red fluorescence of active chlorophyll in the oxygen absorption line at 760 nm, which is directly related to the efficiency of photosynthesis. Thus, the map illustrates the variable photosynthetic rates of the different vegetation types. The highest fluorescence signals come from sugar beets, while other vegetation types were already approaching autumn senescence.

to upscale the water, energy, and CO_2 fluxes in the terrestrial system from the local to the catchment scale based on a numerical approach combined with stochastic techniques. The analysis of the simulations with grids that honor the respective scales reveals the role of flux patterns in the system and helps to design a general upscaling framework that quantifies information transfer between scales due to nonlinear interactions in the system. Accordingly, TR32 uses and develops physics-based process models and model platforms for all relevant scales. For example, pore-scale models using lattice Boltzmann methods have been used for the simulation of multiphase flow in soil pores and the related NMR relaxation behavior (Fig. 4; lattice Boltzmann simulations). These simulations advanced our understanding of NMR observations and helped their interpretation in terms of soil water retention and hydraulic conductivity properties used in hydraulic models (Mohnke and Klitzsch 2010). On a somewhat larger scale (10^{-3}–10^{-2} m), a soil root model was developed to derive improved parameterizations for root density and distribution in the soil, as well as their effect on the soil moisture profiles and respiration as a function of larger-scale soil state variables and parameters (see “Soil root model” for more information). LES models (see below) with highly resolved land surface and subsurface models for energy fluxes, water flow, and carbon dynamics are used for resolving patterns and heterogeneities on numerical grids of the order of centimeters (vertical) to decimeters (horizontal) for land surface and subsurface, while the atmosphere from the LES is assumed homogeneous on this scale. Patterns on scales from tens to several hundred meters, which are mainly characterized by land-use patterns and subsurface structures generated from, for example, geomorphologic processes such as erosion or river evolution, are addressed by simulations with a coupled LES–ALM that is derived from the WRF Model (e.g., Done et al. 2004) and supplemented with a new land surface scheme adapted to the LES resolution (Shao et al. 2013). TerrSysMP (see “TerrSysMP” for more information) is designed for the regional climate scale with resolutions from about 100 meters to kilometers. In TerrSysMP the 3D water cycle is two-way coupled from the free subsurface aquifer to the atmosphere, as, for example, pioneered by Seuffert et al. (2002), but including surface water flow in rivers.

For highly resolved simulations of the 3D water flow in small subcatchments, we apply HGS (e.g., Cornelissen et al. 2014). HGS can be applied on nonrectangular grids, which is particularly useful for small-scale soil, land-use, and topography applications. The comparison of the mean simulated

SOIL ROOT MODEL

Plant roots play an important role in the terrestrial water cycle, as they take up water from the soil that is pumped up back into the atmosphere by plants. Since plant roots increase the depth of the soil layer from which water can be taken up and transpired back into the atmosphere, the depth of the root zone is an important structural feature of terrestrial systems. Root-zone depths depend on the interaction between vegetation, climate, and soil (Schenk and Jackson 2005) and show a seasonal dynamics. The plasticity of root systems to changing environmental conditions is therefore an additional important feature of terrestrial systems. Besides root-zone depths, the root density distribution is also important, since water is expected to be taken up more easily from soil layers with a high root density. The structure of the plant root system therefore has an imprint on soil water distributions, with soil layers with a high root density drying out more rapidly. However, how root water uptake changes when part of the root zone dries out during droughts is a source of uncertainty in models. Neglecting compensatory uptake from deeper soil layers in simulation models is considered to be the reason for the underestimation of transpiration during dry spells (Wang and Dickinson 2012). To improve the prediction of root water uptake dynamics, a biophysical model that couples flow and transport processes in the soil and plant root system while spatially resolving water fluxes to single roots has been developed (Javaux et al. 2008). Simulations by this model (Fig. SB2) were used to infer upscaling rules that can be used to parameterize larger-scale simulation models that do not resolve single plant roots (Javaux et al. 2013; Couvreur et al. 2012). Processes like root growth and regulation of transpiration by hormonal signals that are produced in the root zone as a function of soil environmental conditions have been implemented in the model to investigate whether these processes lead to a fundamentally different behavior of root water uptake. To verify the behavior of the model, two rhizotron facilities have been constructed in the Selhausen area, in which root growth, soil water content, soil water potential, and plant transpiration are noninvasively measured in two different soil types with different water holding capacity and for different water application regimes.

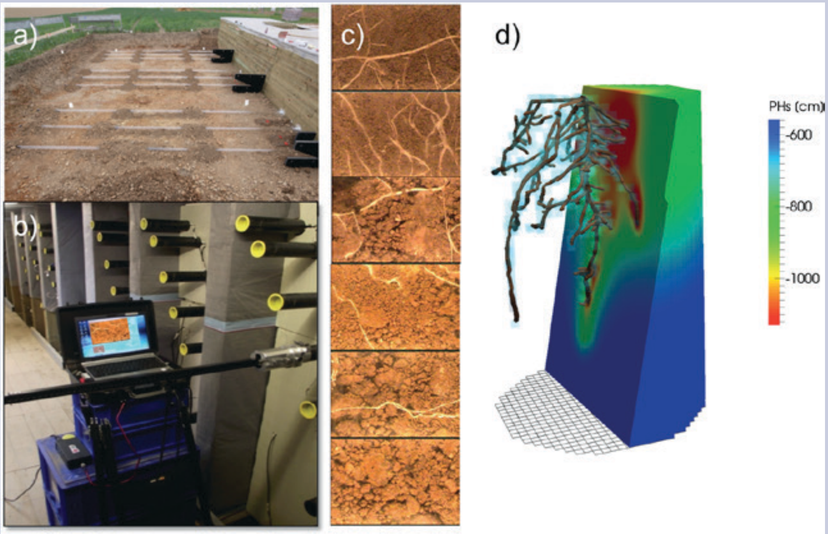

Fig. SB2. (a) Installation of fifty-four 8-m-long transparent rhizotubes (nine at six depths), (b) recording images of roots along rhizotubes using a BTC2 video microscope (Bartz Technology Corporation), (c) examples of recorded images in rhizotubes at different depths from which the evolution of the relative root density distribution during the growing season is derived, and (d) three-dimensional simulation of root water uptake by a root architecture using the coupled soil root model R-SWMS (Javaux et al. 2008): color scale represents the soil water PH, and transparent cyan colors represent water uptake by root segments.

and observed soil moisture dynamics of a 27-ha forested headwater subcatchment of the Rur for the period 2010/2011 (Fig. 5) shows the ability of HGS to capture long-term dynamics in a reasonable manner. The model failed, however, to reproduce short-term dynamics, probably because of a missing preferential flow component (as opposed to matrix flow) in HGS; that is, the treatment of enhanced water flow in soil by, for example, wormholes, root holes, or cracks. The general spatial patterns of simulations and observations are similar (Fig. 6) and are determined by the complex interactions between soil, topography, and vegetation. The subcatchment is currently in a forced transition from a largely fir-dominated forest to a more natural beech-dominated mixed forest. Stable isotope observations are being set up in order to study the ensuing changes in the flow pathways of water in the catchment.

We investigate the propagation of land surface heterogeneity in the atmospheric boundary layer with LES–ALM (Shao et al. 2013), as, for example, suggested by Stevens and Lenschow (2001) and as applied using LES models coupled with land surface schemes (as opposed to fixed surface fluxes)

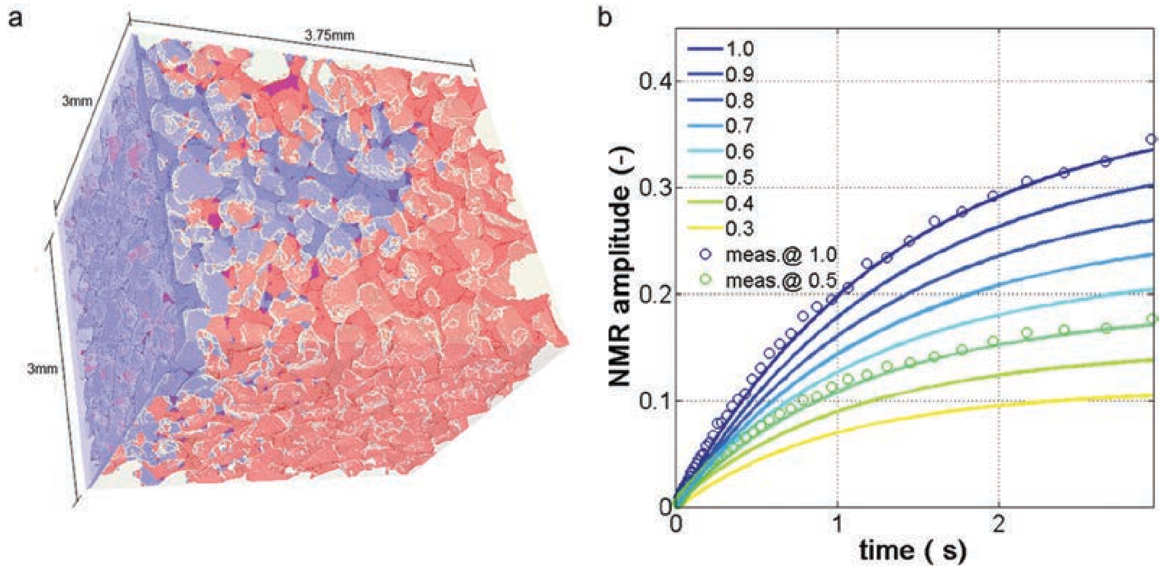

Fig. 4. Lattice Boltzmann simulations at the pore scale: (a) fluid distribution in the pore space of a sand sample (air is blue and water is red) at a water saturation of 0.6 and (b) simulated (lines) and measured (circles) NMR saturation recovery data of the same sample for water saturations between 0.3 and 1 (color coded).

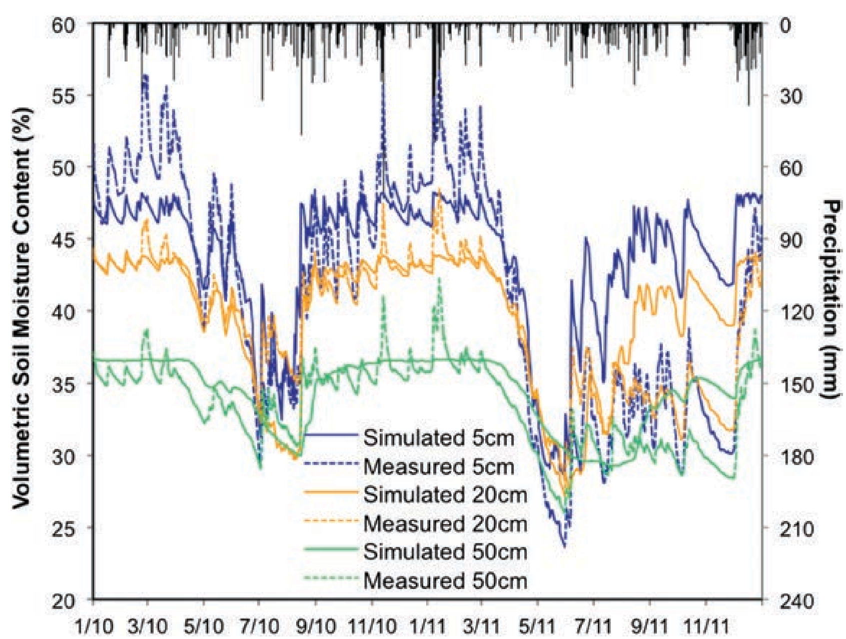

Fig. 5. Mean soil moisture simulation results at different depths (left ordinate) for the 27-ha Wüstebach headwater subcatchment of the Rur catchment (see Fig. 1) at 25-m spatial resolution for the period from the beginning of 2010 to the end of 2011. The black columns protruding from the top abscissa indicate daily precipitation sums (right ordinate). Soil moisture was measured at 150 sites (see Fig. 6) from which 112 were used in this study.

by Patton et al. (2005) and Brunsell et al. (2011), among many others. Liu and Shao (2013) pointed out that the traditional soil-layer configuration adapted from climate models in these studies reacts too slowly to represent atmosphere and land surface feedbacks on large-eddy time scales, a conclusion that led to the development of LES–ALM. Here we present example results for the natural land surface at the Selhausen–Merken field site [for model settings, see Shao et al. (2013)]. The evolution of the patterns of sensible and latent heat fluxes, temperature, humidity, and turbulent kinetic energy in space and time is analyzed using wavelet decomposition and averaging over multiple time scales.

Figure 7 shows the variation of *H* patterns with height simulated with LES–ALM for a convective boundary layer with an inversion at 1.6 km above ground level. The *H* patterns and wavelet energy spectra differ substantially at different heights and for different averaging time intervals. The *H* patterns (and patterns of other quantities, not shown) near the surface bear great similarity to the land-use pattern even without time averaging. At larger heights this resemblance decreases for small averaging time intervals as inherent atmospheric patterns emerge, such as the indication of a hexagonal cell at 512 m. With increased averaging time intervals, however, the land surface patterns can again be identified in the *H* patterns, because the large-scale features of the land surface persist over a considerable depth of the ABL. Mahrt (2000) suggested that microscale (i.e., the scale much smaller than the boundary layer depth) surface heterogeneity does not influence the mean structure of the atmospheric boundary layer, and thus a blending height is assumed above which a surface layer exists, where the Monin–Obukhov similarity theory applies. Our coupled LES and land surface simulations confirm that the mean features of the ABL are not strongly influenced by the heterogeneities on scales much smaller than the boundary layer depth, but the patterns of transport in the ABL can be very different for different heterogeneous surfaces. The wavelet analysis reveals that the persistency of land surface patterns in the atmosphere depends on the scale of those patterns; therefore, it is in general not possible to define a blending height and an inertial boundary layer if the surface heterogeneity is multiscale. Mesoscale motion fields play a role here and will become even more important when land-use patterns correlate with orography (e.g., Grossman et al. 2005). An alternative to bulk parameters, such as a blending height, may be to directly parameterize the flux patterns, if we know how land surface signals propagate in the atmospheric boundary layer. The large-eddy simulation atmosphere and land surface model we developed is of considerable value for developing the concepts and techniques on how such parameterizations can be realized.

Results of the pattern interactions emerging from this effort eventually feed into TerrSysMP (see "TerrSysMP" for more information), which includes a downscaling scheme for predicting near-surface atmospheric variables at the scale of its higher-resolved land surface and subsurface scheme (Schomburg et al. 2010, 2012). The three-step

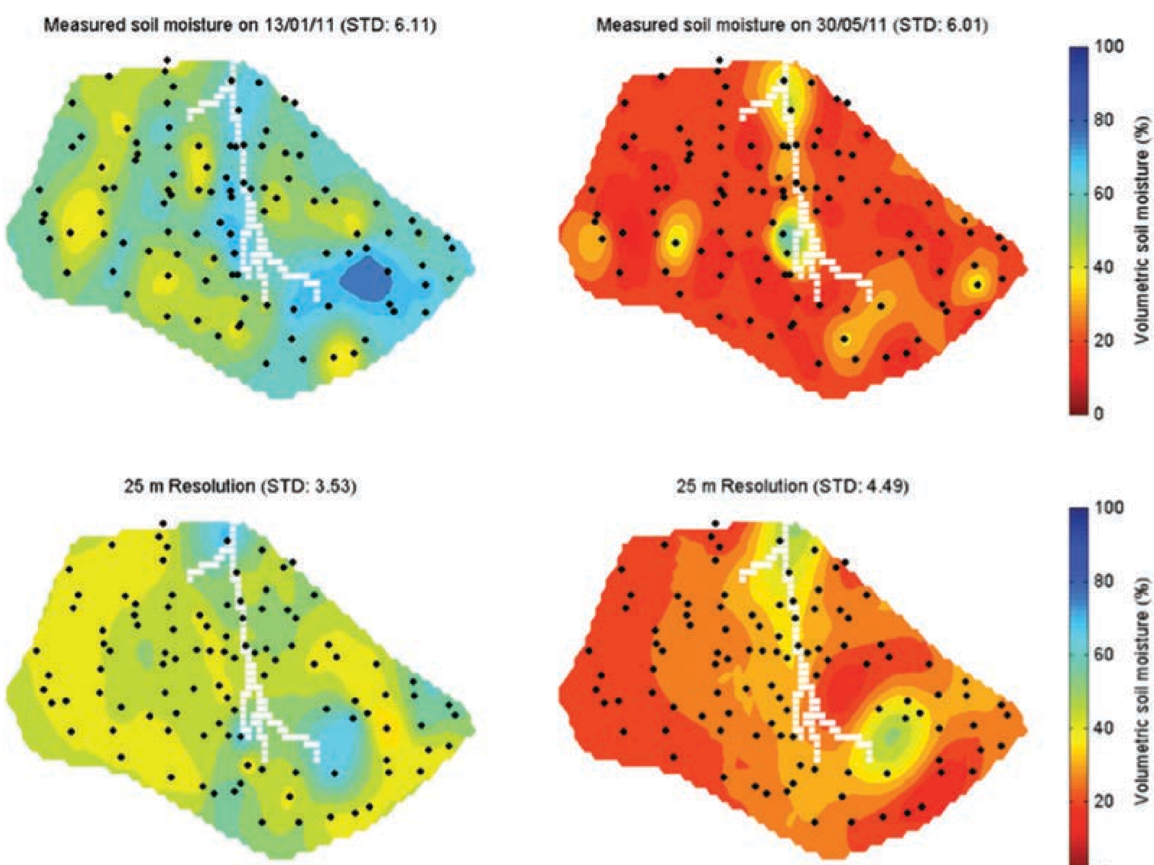

Fig. 6. Spatial distribution of absolute soil moisture for the Wüstebach subcatchment (see Fig. 1) on (left) 13 Jan and (right) 30 May 2011 for (top) measured and (bottom) simulated data for 25-m horizontal resolution. Values in parentheses refer to the mean standard deviation of the kriging algorithm. White lines indicate the streams in the catchment.

downscaling scheme employs spline interpolation while conserving mean and lateral gradients of the coarse field, conditional regression relations between land surface parameters and atmospheric near-surface state variables, and added noise, which restores the variance of the near-surface atmospheric state variables to their expectances. With the second step, we try to capture statistically—besides simple height-dependent extrapolations of profiles in the convective ABL—land surface–driven effects like layer stability and the effects of residual layers within the ABL. The scheme is currently developed further in order to better reproduce special subscale spatiotemporal patterns for example, those produced by cold pools generated in valleys during calm nights. Figure 8 illustrates the performance of a new algorithm based on multiobjective GP. This machine learning method allows checks for physical consistency (in contrast to alternative methods that rely on the output of artificial neural networks) and offers the possibility to quantify the quality of a downscaling rule based on several aspects, such as spatial structure, spatially distributed variance, and spatiotemporal correlation of the fields. Mechanisms for the generation and quantification of such cold pools—as, for example, suggested by LeMone et al. (2003) based on observations—should in principle be detectable by this approach. This downscaling is, however, still limited to the smallest grid size on which TerrSysMP, which applies MOST for the ABL, can be operated with confidence (several hundred meters; work is in progress, however, to implement LES capabilities within TerrSysMP). Patterns currently resolved include differences in land use (bare soil vs cropped soil and differences in crops), soil type, groundwater table depth, and topography.

TerrSysMP simulations with increasing spatial resolution and increasing number of grid cells over the whole Rur area include calculations of both water and carbon dynamics from the subsurface into the atmosphere. Moisture–energy feedbacks at the land surface are well known in the context of

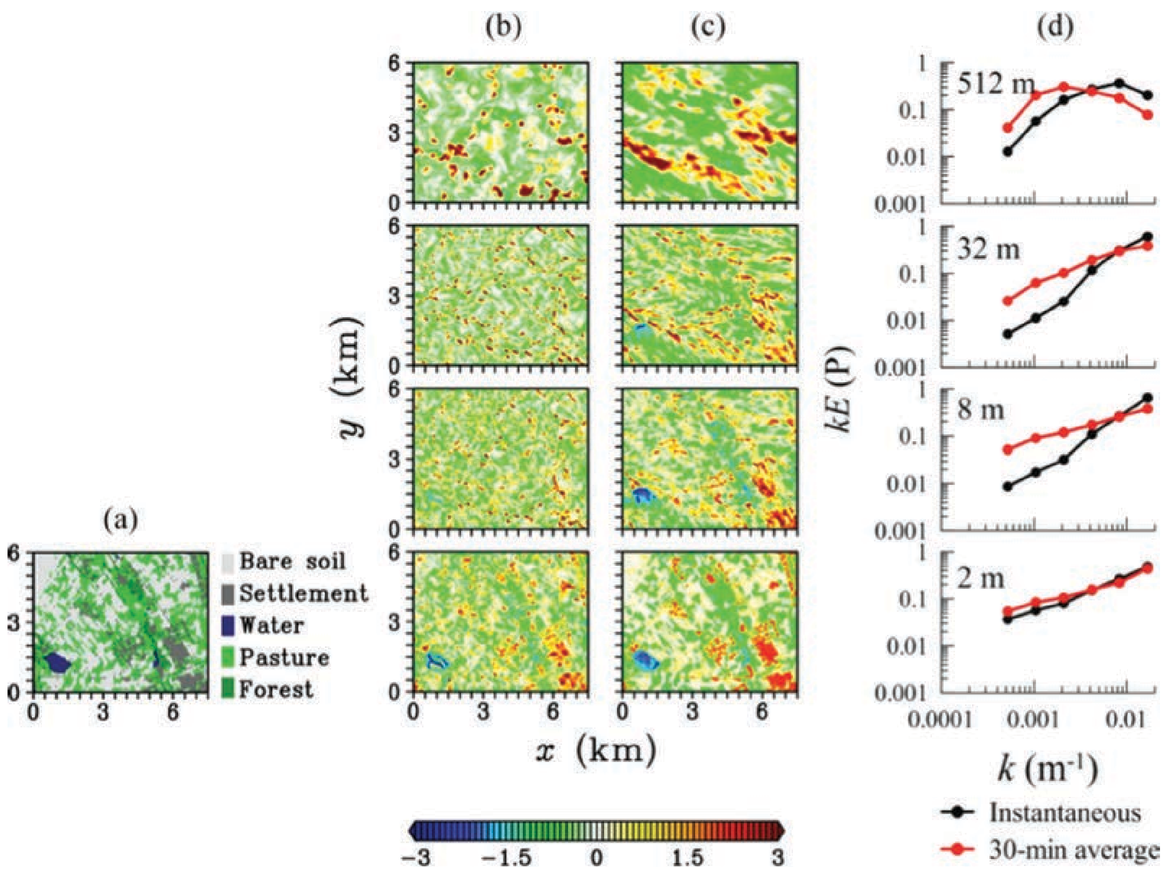

Fig. 7. (a) Land use pattern at the Selhausen–Merken field site. (b) Patterns (deviations from the domain average) of instantaneous sensible heat flux (W m^{-2}) at 1300 UTC 5 Aug 2009, at levels of 2, 8, 32, and 512 m. (c) Patterns of sensible heat flux, but averaged over 30 min. (d) Wavelet energy spectra. Sensible heat fields are Haar decomposed with window sizes of 2, 4, 8, 16, and 32Δx (where Δx = 60 m).

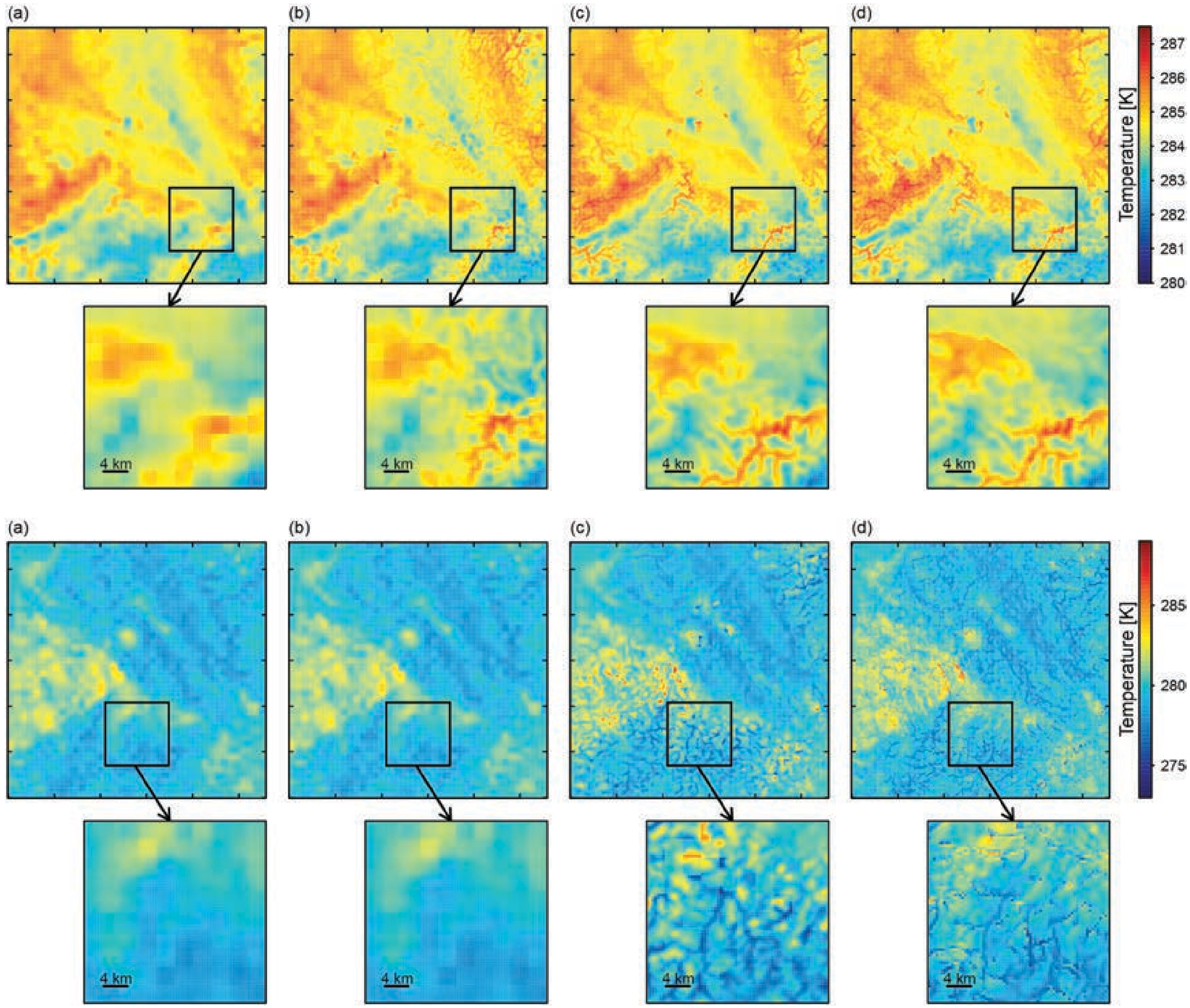

Fig. 8. Disaggregation of the 10-m temperature field (top two rows) at 1200 LT (1100 UTC) and (bottom two rows) at 0000 UTC (2300 UTC) 14 Oct 2007 at 400-m spatial resolution derived from simulation at 2.8-km resolution. The larger squares are fields for an area of 112 km × 112 km and the smaller squares show a subarea of 28 km × 28 km. (a) Spline-interpolated field, (b) field resulting from the downscaling rule by Schomburg et al. (2010), (c) field resulting from the rule found by GP, and (d) reference field from the high-resolution model run at 400 m. In both situations, the GP-based downscaling better reproduces the channel-like, topography-induced patterns in the high-resolution simulations, especially during nighttime conditions. Under the almost clear-sky night in the bottom two rows, temperature inversions cause cold air to drain into the valleys, which leads to pronounced channel structures in the temperature field with substantial variability contained in the fine scales (Zerenner et al. 2014, manuscript submitted to *Environ. Modell. Software*).

water-versus energy-limited landscapes. However, the dominant space and time scales are not well understood where groundwater dynamics dominate the variability of land surface energy fluxes over the atmospheric influence. Using time-localized wavelet spectra (Fig. 9), Rahman et al. (2014) were able to show the coherence of water table dynamics and latent heat at the monthly to multimonth time scale in summer depending on antecedent moisture conditions. Applying similar concepts in the space domain, the simulation results suggest that in summer, the structure in ET is mainly determined by the spatial water table configuration, while ET can be predicted from the spatial structure of R_{net} during cooler months. This hierarchy and interactions of space and time scales is used to derive a theoretical framework to upscale fluxes and to account for the role of patterns, which may include, for example, a coarse graining approach based on wavelets and information theory.

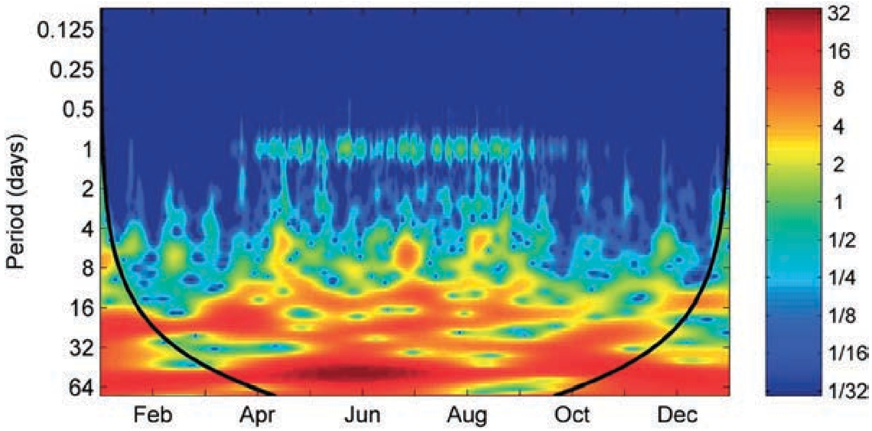

Fig. 9. Cross-wavelet spectrum of latent heat flux at the surface and water table depth simulated by TerrSysMP (CLM coupled to ParFlow and driven with COSMO output) for the year 2009. The cone of influence (results should not be interpreted below this line) is indicated with black lines.

DATA ASSIMILATION. Aside from appropriate boundary conditions, the prediction of the state of the terrestrial system requires knowledge concerning the initial state. Data assimilation—that is, the convolution of observations with a given model state—is the method of choice for this endeavor. In contrast to atmospheric models, terrestrial system models are faced with the additional problem of a priori unknown parameters of the surface, soil, and subsoil, which vary strongly in space and even time due to violations of homogeneity assumptions in the models or even physical hysteresis effects. Thus, parameters need to be included in the data assimilation process. Most observations of the terrestrial system are rather indirect (any remote sensing technique) and depend on additional characteristics of the system, which are often ignored by the terrestrial models because of their minor role in the evolution of the system state variables (e.g., the dependence of the measured neutron intensity by the cosmic-ray probe on litter layers). As many observations as possible should hence be utilized in data assimilation to constrain the very large degree of freedom.

TR32 currently uses LETKF (Hunt et al. 2007) for updating both model state variables and parameters of the land surface model in a column-based approach (Han et al. 2014). The implementation allows assimilating brightness temperature measured by satellites with the CMEM operator (de Rosnay et al. 2009), land surface temperature with a dual-source operator (Kustas and Anderson 2009), and neutron counts with the COSMIC operator (Shuttleworth et al. 2013), besides direct soil moisture and soil temperature measurements (further details are available at http://dx.doi.org/10.1175/BAMS-D-13-00134.3). The catchment-tomography approach, in which localized precipitation events are considered as transmitters and runoff gauges act as integrating receivers, is explored as an alternative approach to determine catchment properties and their impact on water fluxes.

OUTLOOK. With our observation and monitoring capabilities set up and the fully developed integrated terrestrial system models for the meter and kilometer scales in place, the ensuing phase of TR32 will focus on model–data fusion via combined parameter estimation and state-variable assimilation employing DART (Anderson et al. 2009) to address predictability of the terrestrial system on the catchment scale. We plan to include the setup of a flash-flood prediction system in cooperation with a local water management board to demonstrate the immediate applicability of our research-driven efforts for applications. We envision a high-resolution reanalysis dataset of a real mesoscale terrestrial system on the subkilometer scale following the suggestions by Lyon et al. (2008), which we will use to derive budgets of mass and energy for the whole catchment and its major subcatchments for a range of time scales from quasi instantaneous to a decade. The reanalysis dataset is also a basis for the future coupling of water and carbon cycles across different scales and will be of interest for the wider scientific community. TR32 will employ this dataset for the development of an extended view on patterns in terrestrial systems. To reach this goal, we will extend the object-based view currently being developed for the atmospheric sciences for the analysis of, for example, the structure and life cycles of convective systems or atmospheric rivers (e.g., Sellars et al. 2013) to include pattern linkages between the surface and subsurface and structures of the atmospheric boundary layer. This will require the consideration and inclusion of the different time scales on which processes act in the contributing compartments. Following our initial LES-based results on the propagation of patterns from the land surface to the ABL, this requires the consideration of objects living on time scales related to subobjects of the slowest component, like groundwater, carbon pools, or soil moisture. Planned analyses include linking mesoscale motion fields—for example, influenced by persistent surface patterns like the distribution of riparian and upland areas, geomorphological settings, soil orders, or land-use units—with dynamic mass and energy exchange fluxes across the catchment and subcatchment borders, forming a template from which other patterns develop and thereby serving as a key to a better understanding of multiple nonlinear interactions propagating across different temporal and spatial scales.

ACKNOWLEDGMENTS. TR32 has been funded as a Transregional Collaborative Research Center by the Deutsche Forschungsgemeinschaft (DFG) since 2007. Principle investigators of TR32 during its second phase but not appearing in the list of coauthors are A. Bott, C. Burstedde, P. Friederichs, M. Griebel, B. Waske, G. Welp, and M. Van Wijk from the University of Bonn; H. Elbern, P. Fiener, and U. Lang from the University of Cologne; B. Blümich and C. Clauser from Rheinisch-Westfälische Technische Universität Aachen (RWTH Aachen University); A. Graf, M. Herbst, A. Lücke, A. Pohlmeier, L. Weihermüller, and A. Wahner from Forschungszentrum Jülich GmbH; and M. Krafczyk, from Technical University of Braunschweig. The authors acknowledge their essential contributions to TR32 and want to thank all members of TR32 for their dedicated support and enthusiasm for our common goal. Finally, we want to express our great appreciation and thanks to the two anonymous reviewers, who initiated substantial improvements to the paper and also contributed valuable suggestions for the further development of TR32.

APPENDIX: SUMMARY OF ACRONYMS AND VARIABLES

ABL	Atmospheric boundary layer
AERI	Atmospheric Emitted Radiance Interferometer
ATV	All-terrain vehicle
BALTEX BRIDGE	Field experiment during the Baltic Sea Experiment of GEWEX
BoXPol	Bonn X-band polarization radar
CASES	Cooperative Atmosphere–Surface Exchange Study
C band	Radar frequency band between 4 and 8 GHz
CLM	Community Land Model
CMEM	Community Microwave Emission Model
COSMIC	Cosmic-Ray Soil Moisture Interaction Code
COSMO	Consortium for Small-Scale Modeling
CRC	Collaborative research center (institutional structure funded by DFG for up to 12 years)
DART	Data Assimilation Research Testbed
DFG	Deutsche Forschungsgemeinschaft (German national science foundation)
DNS	Direct numerical simulation
DWD	Deutscher Wetterdienst (German national weather service)
EC	Eddy covariance (flux estimation technique)
ECa	Apparent electric conductivity
EMI	Electromagnetic induction
ET	Evapotranspiration
Galileo	Global-satellite-based positioning service provided by several European countries named after Galileo Galilei
GEWEX	Global Energy and Water Exchanges Experiment
GLONASS	Globalnaja Nawigazionnaja Sputnikowaja Sistema (Russian global satellite-based positioning service)
GmbH	Gemeinschaft mit beschränkter Haftung (German company with limited liability)
GP	Genetic programming
GPR	Ground-penetrating radar
H	Sensible heat flux
HyPlant	High-performance imaging spectrometer for estimating sun-induced fluorescence of plants
HGS	HydroGeoSphere (a 3D hydrological model)
JOYCE	Jülich Observatory for Cloud Evolution
JuXPol	Jülich X-band polarization radar
LAI	Leaf area index
LDR	Linear depolarization ratio
LES	Large-eddy simulation
LES–ALM	LES–atmosphere–land surface model

LETKF	Local ensemble transform Kalman filter
LH	Latent heat flux from CLM
l_s	Spatial scale of land surface heterogeneity
l_t	Spatial scale of convective turbulent eddies
LWdn	Longwave downward radiation at the surface
LWup	Longwave upward radiation at the surface
MCT	Model Coupling Toolkit
MIRS	Midinfrared spectroscopy
MRI	Magnetic resonance imaging
MRR	Micro Rain Radar
MLH	mixing-layer height
MOST	Monin–Obukhov similarity theory
NAVSTAR GPS	Navigational Satellite Timing and Ranging global positioning system, a global satellite-based positioning service of the United States
NMR	Nuclear magnetic resonance
OASIS	Ocean Atmosphere Sea Ice Soil
P	en-level air pressure
ParFlow	A parallel, three-dimensional, variably saturated groundwater flow code
PH	Pressure head
q_e	Plant transpiration
q_{rain}	Infiltration
QV	Screen-level specific humidity
RANS	Rayleigh-averaged Navier–Stokes
R_{net}	Surface net radiation
R-SWMS	Root–soil water movement and solute transport
SH	Sensible heat flux from CLM
SIP	Spectral-induced polarization
S_w	Soil moisture content
SW	Shortwave downward radiation at the surface
T	Screen-level temperature
TAU	Friction velocity from CLM
TERENO	Terrestrial Environmental Observatories program of the Helmholtz Association
TerrSysMP	Terrestrial System Modeling Platform
TR32	Transregional 32
τ_a	Averaging time scale
τ_t	Time scale of convective atmospheric eddies
U	Screen-level wind speed
v_D	Doppler velocity
WRF Model	Weather Research and Forecasting Model
WTD	Water table depth
X band	Radar frequency band between 8 and 12 GHz
Z_e	Effective radar reflectivity
σ_D	Doppler velocity variance
Ψ	Pressure head

REFERENCES

Ament, F., and C. Simmer, 2006: Improved representation of land-surface heterogeneity in a non-hydrostatic numerical weather prediction model. *Bound.-Layer Meteor.*, **121,** 153–174, doi:10.1007/s10546-006-9066-4.

Anderson, J., T. Hoar, K. Raeder, H. Liu, N. Collins, R. Torn, and A. Arellano, 2009: The Data Assimilation Research Testbed: A community facility. *Bull. Amer. Meteor. Soc.*, **90,** 1283–1296, doi:10.1175/2009BAMS2618.1.

Avissar, R., and R. A. Pielke, 1989: A parameterization of heterogeneous land surfaces for atmospheric numerical models and its impact on regional meteorology. *Mon. Wea. Rev.,* **117,** 2113–2136, doi:10.1175/1520-0493(1989)117<2113:APOHLS>2.0.CO;2.

Baatz, R., H. R. Bogena, H.-J. Hendricks Franssen, J. A. Huisman, W. Qu, C. Montzka, and H. Vereecken, 2014: Calibration of a catchment scale cosmic-ray soil moisture network: A comparison of three different methods. *J. Hydrol.,* **516,** 231–244, doi:10.1016/j.jhydrol.2014.02.026.

Bak, P., C. Tang, and K. Wiesenfeld, 1988: Self-organizes criticality. *Phys. Rev.,* **38A,** 364–374, doi:10.1103/PhysRevA.38.364.

Baldauf, M., A. Seifert, J. Förstner, D. Majewski, M. Raschendorfer, and T. Reinhardt, 2011: Operational convective-scale numerical weather prediction with the COSMO model: Description and sensitivities. *Mon. Wea. Rev.,* **139,** 3887–3905, doi:10.1175/MWR-D-10-05013.1.

Bear, J., 1988: *Dynamics of Fluids in Porous Media.* Dover Civil and Mechanical Engineering, Dover Publications, 764 pp.

Bejan, A., and S. Lorente, 2006: Constructal theory of generation of configuration in nature and engineering. *J. Appl. Phys.,* **100,** 041301, doi:10.1063/1.2221896.

Bogena, H., M. Herbst, J. A. Huisman, U. Rosenbaum, A. Weuthen, and H. Vereecken, 2010: Potential of wireless sensor networks for measuring soil water content variability. *Vadose Zone J.,* **9,** 1002–1013, doi:10.2136/vzj2009.0173.

——, J. A. Huisman, R. Baatz, H.-J. Hendricks Franssen, and H. Vereecken, 2013: Accuracy of the cosmic-ray soil water content probe in humid forest ecosystems: The worst case scenario. *Water Resour. Res.,* **49,** 5778–5791, doi:10.1002/wrcr.20463.

Bornemann, L., G. Welp, and W. Amelung, 2010: Particulate organic matter at the field scale: Rapid acquisition using mid-infrared spectroscopy. *Soil. Sci. Soc. Amer. J.,* **74,** 1147–1156, doi:10.2136/sssaj2009.0195.

——, M. Herbst, G. Welp, H. Vereecken, and W. Amelung, 2011: Rock fragments control organic carbon pool sizes in agricultural topsoil. *Soil. Sci. Soc. Amer. J.,* **75,** 1898–1907, doi:10.2136/sssaj2010.0454.

Brunsell, N. A., D. B. Mechem, and M. C. Anderson, 2011: Surface heterogeneity impacts on boundary layer dynamics via energy balance partitioning. *Atmos. Chem. Phys.,* **11,** 3403–3416, doi:10.5194/acp-11-3403-2011.

Busch, S., J. van der Kruk, and H. Vereecken, 2014: Improved characterization of fine-texture soils using on-ground GPR full-waveform inversion. *IEEE Trans. Geosci. Remote Sens.,* **52,** 3947–3958, doi:10.1109/TGRS.2013.2278297.

Chen, H. C., V. C. Patel, and S. Ju, 1990: Solutions of Reynolds-averaged Navier-Stokes equations for three-dimensional incompressible flows. *J. Comput. Phys.,* **88,** 305–336, doi:10.1016/0021-9991(90)90182-Z.

Cornelissen, T., B. Diekkrüger, and H. R. Bogena, 2014: Significance of scale and lower boundary condition in the 3D simulation of hydrological processes and soil moisture variability in a forested headwater catchment. *J. Hydrol.,* **516,** 140–153, doi:10.1016/j.jhydrol.2014.01.060.

Couvreur, V., J. Vanderborght, and M. Javaux, 2012: A simple three-dimensional macroscopic root water uptake model based on the hydraulic architecture approach. *Hydrol. Earth Syst. Sci.,* **16,** 2957–2971, doi:10.5194/hess-16-2957-2012.

Crewell, S., and Coauthors 2004: The BALTEX Bridge campaign: An integrated approach for a better understanding of clouds. *Bull. Amer. Meteor. Soc.,* **85,** 1565–1584, doi:10.1175/BAMS-85-10-1565.

Curdt, C., D. Hoffmeister, C. Jekel, G. Waldhoff, and G. Bareth, 2012: Scientific research data management for soil-vegetation-atmosphere data—The TR32DB. *Int. J. Digital Curation,* **7,** 68–80, doi:10.2218/ijdc.v7i2.208.

Damm, A., A. Erler, W. Hillen, M. Meroni, M. E. Schaepman, W. Verhoef, and U. Rascher, 2011: Modeling the impact of spectral sensor configurations on the FLD retrieval accuracy of sun-induced chlorophyll fluorescence. *Remote Sens. Environ.,* **115,** 1882–1892, doi:10.1016/j.rse.2011.03.011.

——, L. Guanter, S. Garbari, W. Verhoef, D. Schläpfer, and M. E. Schaepman, 2014a: Impact of varying irradiance on vegetation indices and chlorophyll fluorescence derived from spectroscopy data. *Remote Sens. Environ.,* **156,** 202–215, doi:10.1016/j.rse.2014.09.031.

——, ——, V. C. E. Laurent, M. E. Schaepman, A. Schickling, and U. Rascher, 2014b: FLD-based retrieval of sun-induced chlorophyll fluorescence from medium spectral resolution airborne spectroscopy data. *Remote Sens. Environ.,* **147,** 256–266, doi:10.1016/j.rse.2014.03.009.

de Rosnay, P., and Coauthors, 2009: AMMA Land Surface Model Intercomparison Experiment coupled to the Community Microwave Emission Model: ALMIP-MEM. *J. Geophys. Res.,* **114,** D05108, doi:10.1029/2008JD010724.

Diederich, M., A. Ryzhkov, C. Simmer, P. Zhang, and S. Troemel, 2015a: Use of specific attenuation for rainfall measurement at X-band radar wavelengths. Part I: Radar calibration and partial beam blockage estimation. *J. Hydrometeor.,* **16,** 487–502, doi:10.1175/JHM-D-14-0066.1.

——, ——, ——, ——, and ——, 2015b: Use of specific attenuation for rainfall measurement at X-band radar wavelengths. Part II: Rainfall estimates and comparison with rain gauges. *J. Hydrometeor.,* **16,** 503–516, doi:10.1175/JHM-D-14-0067.1.

Done, J., C. A. Davis, and M. Weisman, 2004: The next generation of NWP: Explicit forecasts of convection using the Weather Research and Forecasting (WRF) model. *Atmos. Sci. Lett.,* **5,** 110–117, doi:10.1002/asl.72.

Gasper, F., K. Goergen, P. Shrestha, M. Sulis, J. Rihani, M. Geimer, and S. J. Kollet, 2014: Implementation and scaling of the fully coupled Terrestrial Systems Modeling Platform (TerrSysMP v1.0) in a massively parallel supercomputing environment—A case study on JUQUEEN (IBM Blue Gene/Q). *Geosci. Model Dev.,* **7,** 2531–2543, doi:10.5194/gmd-7-2531-2014.

Grossman, R. L., D. Yates, M. A. LeMone, M. L. Wesely, and J. Song, 2005: Observed effects of horizontal radiative surface temperature variations on the atmosphere over a Midwest watershed during CASES 97. *J. Geophys. Res.,* **110,** D06117, doi:10.1029/2004JD004542.

Han, X., H. J. Hendricks Franssen, C. Montzka, and H. Vereecken, 2014: Soil moisture and soil properties estimation in the Community Land Model with synthetic brightness temperature observations. *Water Resour. Res.,* **50,** 6081–6105, doi:10.1002/2013WR014586.

Hasan, S., C. Montzka, C. Rüdiger, M. Ali, H. Bogena, and H. Vereecken, 2014: Soil moisture retrieval from airborne L-band passive microwave using high resolution multispectral data. *J. Photogramm. Remote Sens.,* **91,** 59–71, doi:10.1016/j.isprsjprs.2014.02.005.

Herbst, M., L. Bornemann, A. Graf, G. Welp, H. Vereecken, and W. Amelung, 2012: A geostatistical approach to the field-scale pattern of heterotrophic soil CO_2 emission using covariates. *Biogeochemistry,* **111,** 377–392, doi:10.1007/s10533-011-9661-4.

Hoffmeister, D., G. Waldhoff, C. Curdt, N. Tilly, J. Bendig, and G. Bareth, 2013: Spatial variability detection of crop height in a single field by terrestrial laser scanning. *Precision Agriculture 13,* J. V. Stafford, Ed., Wageningen Academic Publishers, 267–274.

Hunt, B. R., E. J. Kostelich, and I. Szunyogh, 2007: Efficient data assimilation for spatiotemporal chaos: A local ensemble transform Kalman filter. *Physica D,* **230,** 112–126, doi:10.1016/j.physd.2006.11.008.

Javaux, M., T. Schröder, J. Vanderborght, and H. Vereecken, 2008: Use of a three-dimensional detailed modeling approach for predicting root water uptake. *Vadose Zone J.,* **7,** 1079–1088, doi:10.2136/vzj2007.0115.

——, V. Couvreur, J. Vanderborght, and H. Vereecken, 2013: Root water uptake: From three-dimensional biophysical processes to macroscopic modeling approaches. *Vadose Zone J.,* **12,** doi:10.2136/vzj2013.02.0042.

Kemna, A., and Coauthors, 2012: An overview of the spectral induced polarization method for near-surface applications. *Near Surf. Geophys.,* **11,** 453–468, doi:10.3997/1873-0604.2012027.

Kollet S. J., and R. M. Maxwell, 2008: Capturing the influence of groundwater dynamics on land surface processes using an integrated, distributed watershed model. *Water Resour. Res.,* **44,** W02402, doi:10.1029/2007WR006004.

——, ——, C. S. Woodward, S. Smith, J. Vanderborght, H. Vereecken, and C. Simmer, 2010: Proof of concept of regional scale hydrologic simulations at hydrologic resolution utilizing massively parallel computer resources. *Water Resour. Res.,* **46,** W04201, doi:10.1029/2009WR008730.

Kolmogorov, A. N., 1941: The local structure of turbulence in incompressible viscous fluid for very large Reynolds numbers. *Dokl. Akad. Nauk SSSR,* **30,** 301–305.

Korres, W., T. G. Reichenau, and K. Schneider, 2013: Patterns and scaling properties of surface soil moisture in an agricultural landscape: An ecohydrological modeling study. *J. Hydrol.,* **498,** 89–102, doi:10.1016/j.jhydrol.2013.05.050.

Koster, R., and M. Suarez, 1992: Modeling the land surface boundary in climate models as a composite of independent vegetation stands. *J. Geophys. Res.,* **97,** 2697–2715, doi:10.1029/91JD01696.

Koyama, C. N., W. Korres, P. Fiener, and K. Schneider, 2010: Variability of surface soil moisture observed from multitemporal C-Band synthetic aperture radar and field data. *Vadose Zone J.,* **9,** 1014–1024, doi:10.2136/vzj2009.0165.

Kustas, W., and M. Anderson, 2009: Advances in thermal infrared remote sensing for land surface modeling. *Agric. For. Meteor.,* **149,** 2071–2081, doi:10.1016/j.agrformet.2009.05.016.

Langensiepen, M., M. Kupisch, M. T. van Wijk, and F. Ewert, 2012: Analyzing transient closed chamber effects on canopy gas exchange for optimizing flux calculation timing. *Agric. For. Meteor.,* **164,** 61–70, doi:10.1016/j.agrformet.2012.05.006.

——, ——, A. Graf, M. Schmidt, and F. Ewert, 2014: Improving the stem heat balance method for determining sap-flow in wheat. *Agric. For. Meteor.,* **186,** 34–42, doi:10.1016/j.agrformet.2013.11.007.

LeMone, M. A., and Coauthors, 2000: Land–atmosphere interaction research, early results, and opportunities in the Walnut River Watershed in southeast Kansas:

CASES and ABLE. *Bull. Amer. Meteor. Soc.,* **81,** 757–779, doi:10.1175/1520-0477(2000)081<0757:LIRERA>2.3.CO;2.

——, K. Ikeda, R. L. Grossman, and M. Rotach, 2003: Horizontal variability of 2-m temperature at night during CASES 97. *J. Atmos. Sci.,* **60,** 2431–2449, doi:10.1175/1520-0469(2003)060<2431:HVOMTA>2.0.CO;2.

Liu, S., and Y. Shao, 2013: Soil layer configuration requirement for large-eddy atmosphere and land surface coupled modeling. *Atmos. Sci. Lett.,* **14,** 112–117, doi:10.1002/asl2.426.

Loehnert, U., and Coauthors, 2015: JOYCE: Jülich Observatory for Cloud Evolution. *Bull. Amer. Meteor. Soc.,* **96,** 1157–1174, doi:10.1175/BAMS-D-14-00105.1.

Lyon, S. W., and Coauthors, 2008: Coupling terrestrial and atmospheric water dynamics to improve prediction in a changing environment. *Bull. Amer. Meteor. Soc.,* **89,** 1275–1279, doi:10.1175/2008BAMS2547.1.

Mahrt, L., 2000: Surface heterogeneity and vertical structure of the boundary. *Bound.-Layer Meteor.,* **96,** 33–62, doi:10.1023/A:1002482332477.

Mellor, G. L., and T. Yamada, 1982: Development of a turbulence closure model for geophysical fluid problems. *Rev. Geophys.,* **20,** 851–875, doi:10.1029/RG020i004p00851.

Mengelkamp, H.-T., and Coauthors, 2006: Evaporation over a heterogeneous land surface: The EVA_GRIPS project. *Bull. Amer. Meteor. Soc.,* **87,** 775–786, doi:10.1175/BAMS-87-6-775.

Mester, A., J. van der Kruk, E. Zimmermann, and H. Vereecken, 2011: Quantitative two-layer conductivity inversion of multi-configuration electromagnetic induction measurements. *Vadose Zone J.,* **10,** 1319–1330, doi:10.2136/vzj2011.0035.

Mohnke, O., and N. Klitzsch, 2010: Microscale simulations of NMR relaxation in porous media considering internal field gradients. *Vadose Zone J.,* **9,** 846–857, doi:10.2136/vzj2009.0161.

Monin, A. S., and A. M. Obukhov, 1954: Basic laws of turbulent mixing in the atmosphere near the ground. *Tr. Geofiz. Inst., Akad. Nauk SSSR,* **151,** 163–187.

Oleson, K. W., and Coauthors, 2008: Improvements to the Community Land Model and their impact on the hydrological cycle. *J. Geophys. Res.,* **113,** G01021, doi:10.1029/2007JG000563.

Patton, E. G., P. P. Sullivan, and C.-H. Moeng, 2005: The influence of idealized heterogeneity on wet and dry planetary boundary layers coupled to the land surface. *J. Atmos. Sci.,* **62,** 2078–2097, doi:10.1175/JAS3465.1.

Perlo, J., E. Danieli, J. Perlo, B. Blümich, and F. Casanova, 2013: Optimized slim-line logging NMR tool to measure soil moisture in situ. *J. Magn. Reson.,* **233,** 74–79, doi:10.1016/j.jmr.2013.05.004.

Rahman, M., M. Sulis, and S. Kollet, 2014: The concept of dual-boundary forcing in land surface-subsurface interactions of the terrestrial hydrologic and energy cycles. *Water Resour. Res.,* **50,** 8531–8548, doi:10.1002/2014WR015738.

Richards, L. A., 1931: Capillary conduction of liquids through porous mediums. *Physics,* **1,** 318–333, doi:10.1063/1.1745010.

Rosenbaum, U., H. R. Bogena, M. Herbst, J. A. Huisman, T. J. Peterson, A. Weuthen, A. W. Western, and H. Vereecken, 2012: Seasonal and event dynamics of spatial soil moisture patterns at the small catchment scale. *Water Resour. Res.,* **48,** W10544, doi:10.1029/2011WR011518.

Rudolph, S., J. van der Kruk, C. von Hebel, M. Ali, M. Herbst, C. Montzka, S. Pätzold, D. A. Robinson, H. Vereecken, and L. Weihermüller, 2015: Linking satellite derived LAI patterns with subsoil heterogeneity using large-scale ground-based electromagnetic Induction measurements. *Geoderma,* **241–242,** 262–271, doi:10.1016/j.geoderma.2014.11.015.

Ryzhkov, A., M. Diederich, P. Zhang, and C. Simmer, 2014: Potential utilization of specific attenuation for rainfall estimation, mitigation of partial beam blockage, and radar networking. *J. Atmos. Oceanic Technol.,* **31,** 599–619, doi:10.1175/JTECH-D-13-00038.1.

Schenk, H. J., and R. B. Jackson, 2005: Mapping the global distribution of deep roots in relation to climate and soil characteristics. *Geoderma,* **126,** 129–140, doi:10.1016/j.geoderma.2004.11.018.

Schomburg, A., V. Venema, R. Lindau, F. Ament, and C. Simmer, 2010: A downscaling scheme for atmospheric variables to drive soil–vegetation–atmosphere transfer models. *Tellus,* **62B,** 242–258, doi:10.1111/j.1600-0889.2010.00466.x.

——, ——, ——, ——, and ——, 2012: Disaggregation of screen-level variables in a numerical weather prediction model with an explicit simulation of subgrid-scale land-surface heterogeneity. *Meteor. Atmos. Phys.,* **116,** 81–94, doi:10.1007/s00703-012-0183-y.

Schween, J. H., S. Crewell, and U. Löhnert, 2011: Horizontal-humidity gradient from one single-scanning microwave radiometer. *IEEE Geosci. Remote Sens. Lett.,* **8,** 336–340, doi:10.1109/LGRS.2010.2072981.

Sellars, S., P. Nguyen, W. Chu, X. Gao, K. Hsu, and S. Sorooshian, 2013: Computational Earth science: Big data transformed into insight. *Eos, Trans. Amer. Geophys. Union,* **94,** 277–279, doi:10.1002/2013EO320001.

Seuffert, G., P. Gross, C. Simmer, and E. F. Wood, 2002: The influence of hydrologic modeling on the predicted local weather: Two-way coupling of a mesoscale weather prediction model and a land surface hydrologic model. *J. Hydrometeor.,* **3,** 505–523, doi:10.1175/1525-7541(2002)003<0505:TIOHMO>2.0.CO;2.

Shao, Y., S. Liu, J. H. Schween, and S. Crewell, 2013: Large-eddy atmosphere–land-surface modelling over heterogeneous surfaces: Model development and comparison with measurements. *Bound.-Layer Meteor.,* **148,** 333–356, doi:10.1007/s10546-013-9823-0.

Shrestha, P., M. Sulis, M. Masbou, S. Kollet, and C. Simmer, 2014: A scale-consistent Terrestrial System Modeling Platform based on COSMO, CLM and ParFlow. *Mon. Wea. Rev.,* **142,** 3466–3483, doi:10.1175/MWR-D-14-00029.1.

Shuttleworth, J., R. Rosolem, M. Zreda, and T. E. Franz, 2013: The COsmic-ray Soil Moisture Interaction Code (COSMIC) for use in data assimilation. *Hydrol. Earth Syst. Sci.,* **17,** 3205–3217, doi:10.5194/hess-17-3205-2013.

Stevens, B., and D. Lenschow, 2001: Observations, experimental and large eddy simulation. *Bull. Amer. Meteor. Soc.,* **82,** 283–294, doi:10.1175/1520-0477(2001)082<0283:OEALES>2.3.CO;2.

Sulis, M., M. Langensiepen, P. Shrestha, A. Schickling, C. Simmer, and S. J. Kollet, 2015: Evaluating the influence of plant-specific physiological parameterizations on the partitioning of land surface energy fluxes. *J. Hydrometeor.,* **16,** 517–533, doi:10.1175/JHM-D-14-0153.1.

Valcke, S., and Coauthors, 2012: Coupling technologies for Earth System Modelling. *Geosci. Model Dev.,* **5,** 1589–1596, doi:10.5194/gmd-5-1589-2012.

——, T. Craig, and L. Coquart, Eds., 2013: OASIS3-MCT user guide: OASIS3-MCT 2.0. CERFACS Tech. Rep. TR/CMGC/13/17, CERFACS/CNRS SUC URA 1875, 50 pp. [Available online at http://pantar.cerfacs.fr/globc/publication/technicalreport/2013/oasis3mct_UserGuide.pdf.]

van der Tol, C., W. Verhoef, J. Timmermans, A. Verhoef, and Z. Su, 2009: An integrated model of soil-canopy spectral radiances, photosynthesis, fluorescence, temperature and energy balance. *Biogeosciences,* **6,** 3109–3129, doi:10.5194/bg-6-3109-2009.

Vereecken, H., S. Kollet, and C. Simmer, 2010: Patterns in soil–vegetation–atmosphere systems: Monitoring, modeling, and data assimilation. *Vadose Zone J.,* **9,** 821–827, doi:10.2136/vzj2010.0122.

von Hebel, C., S. Rudolph, A. Mester, J. A. Huisman, P. Kumbhar, H. Vereecken, and J. van der Kruk, 2014: Three-dimensional imaging of subsurface structural patterns using quantitative large-scale multiconfiguration electromagnetic induction data. *Water Resour. Res.,* **50,** 2732–2748, doi:10.1002/2013WR014864.

Wang, K. C., and R. E. Dickinson, 2012: A review of global terrestrial evaporation: Observation, modelling, climatology, and climatic variability. *Rev. Geophys.,* **50,** RG2005, doi:10.1029/2011RG000373.

Zacharias, S., and Coauthors, 2011: A network of terrestrial environmental observatories in Germany. *Vadose Zone J.,* **10,** 955–973, doi:10.2136/vzj2010.0139.

Zreda, M., D. Desilets, T. P. A. Ferré, and R. L. Scott, 2008: Measuring soil moisture content non-invasively at intermediate spatial scale using cosmic-ray neutrons. *Geophys. Res. Lett.,* **35,** L21402, doi:10.1029/2008GL035655.

AMS BOOKS

RESEARCH ◆ APPLICATIONS ◆ HISTORY

AMS MEMBERS GET FREE

CLIMATE

The Thinking Person's Guide to Climate Change

ROBERT HENSON

This fully updated and expanded revision of The *Rough Guide to Climate Change* combines years of data with recent research. It is the most comprehensive overview of climate science, acknowledging controversies but standing strong in its stance that the climate is changing—and something needs to be done.

© 2014, PAPERBACK, 520 PAGES,
ISBN: 978-1-935704-73-7
LIST $30 MEMBER $20

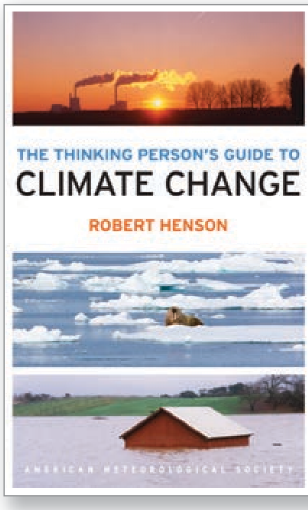

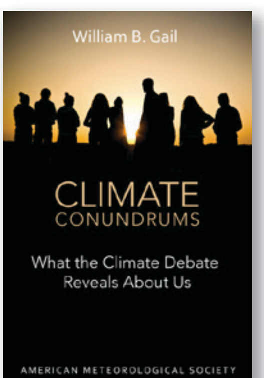

Climate Conundrums:
What the Climate Debate Reveals about Us

WILLIAM B. GAIL

This is a journey through how we think, individually and collectively, about humanity's relationship with nature, and more. Can we make nature better? Could science and religion reconcile? Gail's insights on such issues help us better understand who we are and find a way forward.

© 2014, PAPERBACK, 240 PAGES,
ISBN: 978-1-935704-74-4 LIST $30 MEMBER $20

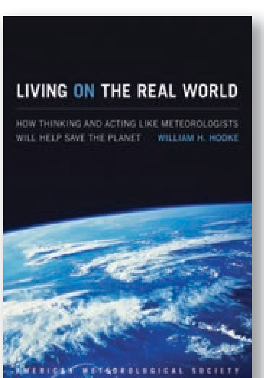

Living on the Real World:
How Thinking and Acting Like Meteorologists Will Help Save the Planet

WILLIAM H. HOOKE

Meteorologists focus on small bits of information while using frequent collaboration to make decisions. With climate change a reality, William H. Hooke suggests we look to the way meteorologists operate as a model for how we can solve the 21st century's most urgent environmental problems.

© 2014, PAPERBACK, 272 PAGES, ISBN 978-1-935704-56-0 LIST $30 MEMBER $22

GUIDES

An Observer's Guide to Clouds and Weather:
A Northeastern Primer on Prediction

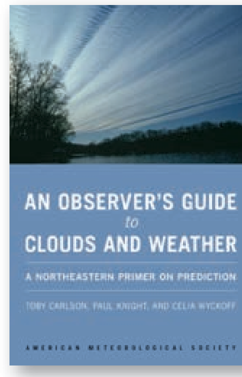

TOBY CARLSON, PAUL KNIGHT, AND CELIA WYKOFF

With help from Penn State experts, start at the beginning and go deep. This primer, intended for both serious enthusiasts and new meteorology students, will leave you with both refined observation skills and an understanding of the complex science behind the weather: the ingredients for making reliable predictions of your own. It connects fundamental meteorological concepts with the processes that shape weather patterns, and will make an expert of any dedicated reader.

© 2014, PAPERBACK, 210 PAGES,
ISBN: 978-1-935704-58-4 LIST $30 MEMBER $20

Eloquent Science:
A Practical Guide to Becoming a Better Writer, Speaker, and Atmospheric Scientist

DAVID M. SCHULTZ

The ultimate communications manual for undergraduate and graduate students as well as researchers in the atmospheric sciences and their intersecting disciplines.

© 2009, PAPERBACK, 440 PAGES,
ISBN 978-1-878220-91-2

LIST $45 MEMBER $30

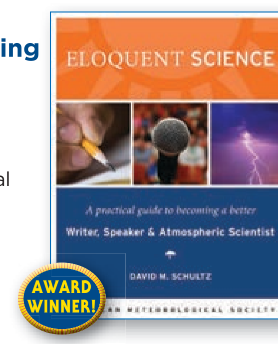

TEXTBOOK

Midlatitude Synoptic Meteorology:
Dynamics, Analysis, and Forecasting

GARY LACKMANN

This textbook links theoretical concepts to modern technology, facilitating meaningful application of concepts, theories, and techniques using real data.

©2011, PAPERBACK, 360 PAGES,
ISBN 978-1-878220-10-3
LIST $100 MEMBER $75 STUDENT MEMB. $65

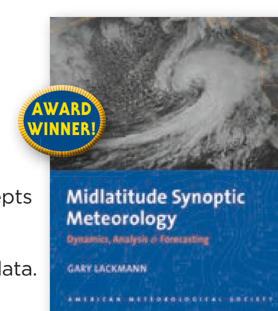

Midlatitude Synoptic Meteorology Teaching CD
More than 1,000 PowerPoint Slides.
© 2013, CD, ISBN 978-1-878220-27-1 LIST $100 MEMBER $75

To order: bookstore.ametsoc.org, 617-226-3998, or use the order form in this magazine

SHIPPING + DISCOUNTS AT BOOKSTORE.AMETSOC.ORG

COMING SOON!

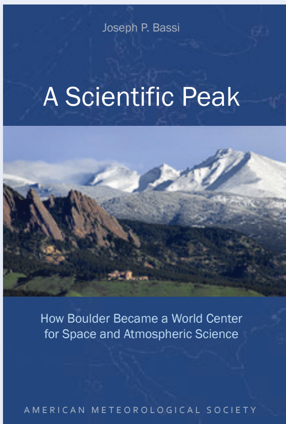

A Scientific Peak:
How Boulder Became a World Center for Space and Atmospheric Science

JOSEPH P. BASSI

How did big science come to Boulder, Colorado? Joe Bassi introduces us to the characters, including Harvard sun–Earth researcher Walter Orr Roberts, and the unexpected brew of politics, passion, and sheer luck that during the Cold War era transformed this "Scientific Siberia" to home of NCAR and NOAA.

METEOROLOGICAL MONOGRAPH SERIES

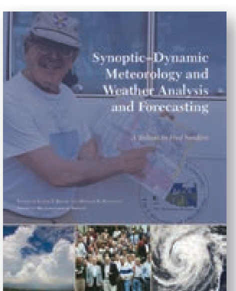

Synoptic–Dynamic Meteorology and Weather Analysis and Forecasting:
A Tribute to Fred Sanders

EDITED BY LANCE F. BOSART AND HOWARD B. BLUESTEIN

© 2008, HARDCOVER, 440 PAGES, VOL. 33, NO. 55, ISBN 978-1-878220-84-4

LIST $120 MEMBER $80
STUDENT MEM. $60

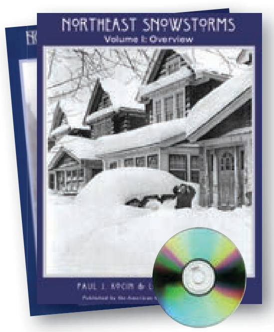

Northeast Snowstorms
(Volume I: Overview, Volume II: The Cases)

PAUL J. KOCIN AND LOUIS W. UCCELLINI

© 2004, TWO HARDCOVER VOLS. PLUS DVD, VOL. 32, NO. 54, ISBN 978-1-878220-64-6

LIST $100 MEMBER $80
STUDENT MEM. $60

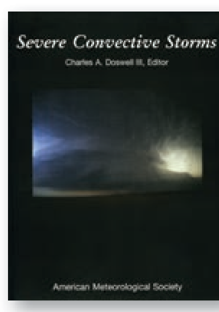

Severe Convective Storms

EDITED BY CHARLES A. DOSWELL III

© 2001, HARDCOVER, 570 PAGES, VOL. 28, NO. 50, ISBN 978-1-878220-41-7

LIST $110 MEMBER $90
STUDENT MEM. $75

Booksellers, groups, or for examination copies:
The University of Chicago Press:
1-800-621-2736 (US & Canada)
773-702-7000 (all others)
custserv@press.uchicago.edu

NOTIFICATION OF NEW AMS TITLES: www.ametsoc.org/JOIN

HISTORY

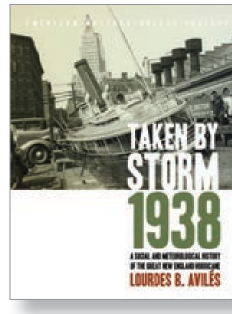

Taken by Storm, 1938:
A Social and Meteorological History of the Great New England Hurricane

LOURDES B. AVILÉS

The science behind the 1938 Hurricane, which hit New England unannounced, is presented here for the first time along with new data that sheds light on the motivations of the Weather Bureau forecasters. This compelling history successfully weaves science, historical accounts, and social analyses to create a comprehensive picture of the most powerful and devastating hurricane to hit New England to date.

© 2013, HARDCOVER, 288 PAGES, ISBN: 978-1-878220-37-0

LIST $40 MEMBER $30

Father Benito Viñes:
The 19th-Century Life and Contributions of a Cuban Hurricane Observer and Scientist

LUIS E. RAMOS GUADALUPE
TRANSLATED BY OSWALDO GARCIA

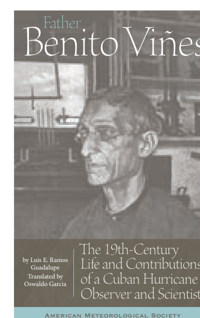

Before Doppler radar and weather broadcasts, Spanish Jesuit Benito Viñes (1837–1893) spent decades observing the skies at Belen Observatory in colonial Cuba. Nicknamed "the Hurricane Priest," Viñes taught the public about the weather and developed the first network of weather observation stations in the Caribbean, groundwork for the hurricane warning systems we use today.

© 2014, PAPERBACK, 172 PAGES
ISBN: 978-1-935704-62-1 LIST $20 MEMBER $16

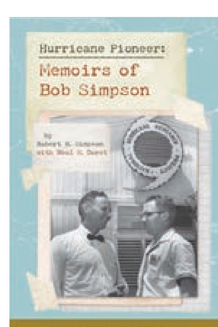

Hurricane Pioneer:
Memoirs of Bob Simpson

ROBERT H. SIMPSON AND NEAL DORST

In 1951, Bob Simpson rode a plane into a hurricane—just one of the many pioneering exploits you'll find in these memoirs. Bob and his wife Joanne are meteorological icons: Bob was the first director of the National Hurricane Research Project and a director of the National Hurricane Center. He helped to create the Saffir–Simpson Hurricane Scale; the public knows well his Categories 1–5. Proceeds from this book help support the AMS's K. Vic Ooyama Scholarship Fund.

© 2015, PAPERBACK, 156 PAGES
ISBN: 978-1-935704-75-1 LIST $25 MEMBER $20

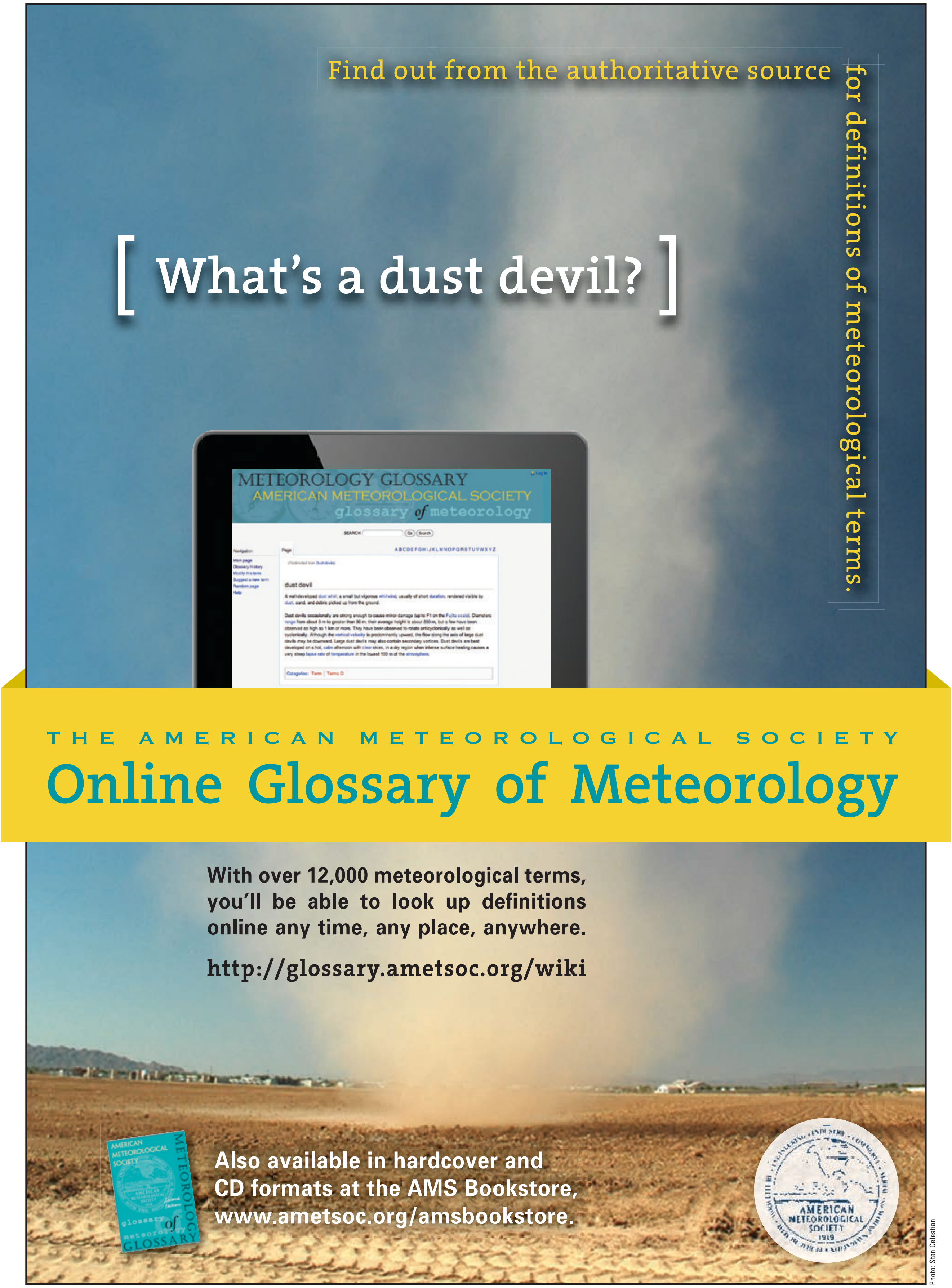

Photo: Stan Celestian